MIRD Pamphlet No. 14 Revised: A Dynamic Urinary Bladder Model for Radiation Dose Calculations

Stephen R. Thomas, Michael G. Stabin, Chin-Tu Chen and Ranasinghage C. Samaratunga

A Task Group of the MIRD Committee, Society of Nuclear Medicine
Department of Radiology, University of Cincinnati College of Medicine, Cincinnati, Ohio; Oak Ridge Associated Universities, Oak Ridge, Tennessee; and University of Chicago, Chicago, Illinois

The constant-volume urinary bladder model in the standard MIRD Pamphlet No. 5 (Revised) phantom has recognized limitations. Various investigators have developed detailed models incorporating more physiologically realistic features, such as expanding bladder contents and residual volume, and variable urinary input rate, initial volume and first void time. We have reviewed these published models and have developed a new model for calculation of radiation absorbed dose to the urinary bladder wall incorporating these aspects. **Methods:** The model consists of a spherical source with variable volume to simulate the bladder contents and a wall represented by a spherical shell of constant volume. The wall thickness varies as the source expands or contracts. The model provides for variable urine entry rate (three different hydration states), initial bladder contents volume, residual volume and first void time. The voiding schedule includes an extended nighttime gap during which the urine entry rate is reduced to one-half the daytime rate. **Results:** Radiation-absorbed dose estimates have been calculated for the bladder wall surface (including photon and electron components) and at several depths in the wall (electron component) for 2-^{18}F-fluoro-2-deoxy-D-glucose, ^{99m}Tc-diethylenetriaminepentaacetic acid (DTPA), ^{99m}Tc-HEDP, ^{99m}Tc-pertechnetate, ^{99m}Tc-red blood cells (RBCs), ^{99m}Tc-glucoheptonate, ^{99m}Tc-mercaptoacetyltriglicine chelator (MAG3), ^{99m}Tc-methylene diphosphonate (MDP), ^{99m}Tc-hexamethylpropylene amine oxime (HMPAO), ^{99m}Tc-human serum albumin (HSA), ^{99m}Tc-MIBI (rest and stress), ^{123}I-/^{124}I-/^{131}I-OIH, ^{123}I/^{131}I-NaI, ^{125}I-iothalamate, ^{111}In-DTPA and ^{89}Sr-SrCl. **Conclusion:** The new model tends to give a higher radiation absorbed dose to the bladder wall surface than the previous models. Large initial bladder volumes and higher rates of urine flow into the bladder result in lower bladder wall dose. The optimal first voiding time is from 40 min to 3 hr postadministration, depending on radiopharmaceutical. The data as presented in tabular and graphic form for each compound provide guidance for establishing radiation absorbed dose reduction protocols.

Key Words: dosimetry; urinary bladder radiation absorbed dose; dynamic bladder; MIRD dose calculation

J Nucl Med 1999; 40:102S–123S

FOREWORD TO REVISED MIRD PAMPHLET NO. 14

The theoretical concepts and output calculations for the radiation absorbed dose to the urinary bladder wall were published originally as MIRD Pamphlet No. 14, "A Dynamic Urinary Bladder Model for Radiation Dose Calculations" (*1*). After publication, the authors discovered an error in the computer code used to generate the output values, which introduced an error in the calculated results with a magnitude dependent on the radionuclide as well as the specific model parameters. The values published originally were ~40% low (ranging from < 10% low to > 60% low). In addition, typographical errors were identified in the expressions involving the model description. The MIRD Committee recognized the importance of rectifying this situation and announced the preparation of a revised pamphlet (*2*), which would provide corrections and also take the opportunity to expand the list of radiopharmaceuticals presented. The requisite corrections and changes have been implemented in this revision along with the inclusion of eight additional radiopharmaceuticals thus providing results for a total of 19 agents used both diagnostically and therapeutically. For some of the original radiopharmaceuticals, the biologic parameters have been updated through new references and/or revised kinetic modeling analysis, which also has introduced modifications in the calculated results.

INTRODUCTION

Calculation of radiation absorbed dose (hereafter referred to as "radiation dose" or simply "dose"') to the inner mucosal surface and at depth in the urinary bladder wall from radioactivity distributed within the bladder contents is of importance for:

1. Evaluating new or existing radiopharmaceuticals for human use; and
2. Designing patient protocol strategies intended to minimize the radiation dose for a specific radiopharmaceutical.

Accurate radiation dose estimates may hold particular significance for those agents that are excreted rapidly, such as 2-^{18}F-fluoro-2-deoxy-D-glucose (FDG) (*3,4*) and ^{99m}Tc-diethylenetriaminepentaacetic acid (DTPA) (*4*).

Most dose estimates to the bladder wall are based on the standard MIRD 5 (Revised) phantom, in which the bladder has a constant volume (*5*). No provision is made for dynamic variation or incorporation of other variables (such as filling rate, initial volume, residual volume, first voiding time and wall thinning) that may be expected to have an effect on the dose. The limitations of this bladder model have long been recognized and various alternative models have been proposed. In this paper, the published models for the urinary bladder are reviewed, and the results are compared with those provided under equivalent conditions by the original MIRD model. A new model was developed that incorporates the complexities of

Received Feb. 26, 1998; revision accepted Jun. 29, 1998.
For correspondence contact: Stephen R. Thomas, PhD, E560 Medical Sciences Building, University of Cincinnati, College of Medicine, Cincinnati, OH 45267-0579.
For reprints contact: Evelyn E. Watson, MS, Chair, MIRD Committee, 104 New Bedford Lane, Oak Ridge, TN 37830.
This is the last in a series of MIRD Special Contributions.

TABLE 1
Definition of Symbols Used in the Calculational Methods Described in Table 2

Symbol	Name/description	Units*	
		Traditional	S.I.
$\tilde{A}$	Cumulated activity, $\tilde{A} = \int A(t)dt$	μCi · h	MBq · s
A(t)	Activity within the bladder at time t	μCi (or mCi)	MBq
$A_v(t)$	Bladder activity per unit volume at time t	$\mu Ci/cm^3$ (or mCi/cm^3)	MBq/cm^3
$\bar{D}/A_0$ $[D_s/A_0]$	Average dose to the bladder wall [or dose to the inner surface] per unit administered activity	rad/μCi (or rad/mCi)	mGy/MBq
$D_\gamma(V)$	Photon dose to the bladder wall at bladder volume V	rad	mGy
$f[f_i]$	Residual bladder volume fraction following a void [the i^th^ void]	—	—
g_s	Geometrical factor for a point on the surface of a sphere	cm	cm
r(t)	Bladder radius at time t	cm	cm
$R_{\beta S}$	Electron dose rate at the bladder wall inner surface per unit activity in the bladder contents volume	rad/mCi · h	mGy/MBq · s
$R_{\gamma S}$	Photon (gamma) dose rate at the bladder wall inner surface per unit activity in the bladder contents volume	rad/mCi · h	mGy/MBq · s
$R_{\gamma W}$	Average photon (gamma) dose rate within the bladder wall per unit activity in the bladder contents volume	rad/mCi · h	mGy/MBq · s
S	S value for the bladder contents (source) to the bladder wall (target)	rad/μCi · h	mGy/MBq · s
T_v	Regular voiding interval	h	s
T_i	Void time for the i^{th} void	h	s
T_1	Time of first void	h	s
U(t)	Urine volume rate of entry into the bladder	ml/min (or cm^3/min)	ml/s (or cm^3/s)
V(t)	Bladder volume at time t	ml (or cm^3)	ml (or cm^3)
$V(T_i)$	Bladder volume prior to i^{th} void at time T_i	ml (or cm^3)	ml (or cm^3)
V_0	Initial bladder contents volume	ml (or cm^3)	ml (or cm^3)
V_r	Residual volume following void	ml (or cm^3)	ml (or cm^3)
X(t)	Gamma ray exposure rate at the inner bladder wall surface at time t	R/h	C/kg · s
α_j	Biologic coefficients representing the fraction of the administered activity entering the bladder for the j^{th} component	—	—
Δ_β	Mean electron particle energy emitted per nuclear transition (formerly equilibrium dose constant)	rad · g/μCi · h	mGy · kg/MBq · s
λ_j	Biologic rate constant for entry of the j^{th} component into the bladder	h^{-1}	s^{-1}
λ	Physical decay constant	h^{-1}	s^{-1}
ρ	Density of the medium	g/ml (or gm/cm^3)	g/cm^3
τ	Residence time in the bladder contents	h	s
Γ	Exposure rate constant	R · cm^2/mCi · h	C · cm^2/kg · MBq · s
Γ'	Exposure rate constant converted to dose in tissue using the roentgen-to-rad or coulomb/kg-to-mGy conversion factor	rad · cm^2/mCi · h	mGy · cm^2/MBq · s
μ	Effective photon absorption coefficient for water at a given energy	cm^{-1}	cm^{-1}

*Care must be taken to use the correct conversion factors (h or s to min, μCi to mCi, g to kg and so on) when applying the units in Table 1 to Equations 1–3 (see Calculational Methods).

urinary function into a practical algorithm for calculating the radiation dose to the bladder wall.

REVIEW OF PREVIOUSLY PUBLISHED URINARY BLADDER MODELS FOR DOSIMETRY CALCULATIONS

Table 1 contains definitions of symbols used in the algorithms of four previously published urinary bladder models for dose calculations that are described in Table 2, along with the new model. Model A in Table 2 is associated with the standard MIRD 5 (Revised) phantom (*5*). [Other information that is relevant to the MIRD schema and model descriptions are provided in references (*6–10*).] A limitation of the model is that the volume of the bladder contents remains constant at 202.6 ml (200 g). The surface electron dose rate is derived from the approximation that the dose rate at the surface of a large sphere is one-half of the dose rate in an infinite medium that has the same radioactive concentration as within the sphere (*11*). The photon dose is derived using Monte Carlo techniques. Bladder wall dose per unit cumulated activity in various source organs, including bladder contents, has been calculated for many radionuclides with this model (*10*). Cumulated activity in bladder contents is derived using a bladder radioactivity input model, which is generally obtained from the whole-body retention curve determined through knowledge of the pharmaceutical biokinetics. No attempt is made to represent the physical dynamics of bladder filling and emptying.

Snyder and Ford (*12*) developed a model in which the bladder is represented as an ellipsoid with axes in the ratio of 4:3:3 (left–right:front–back:top–bottom) that remains fixed as the bladder fills (Model B in Table 2). The surface electron dose rate is also derived using the assumption that the dose rate at the surface of a sphere is one-half of the dose rate in the infinite medium. The variation of electron dose rate with depth is estimated using an integration of Berger's (*13,14*) point kernel for an infinite slab of finite thickness with a semi-infinite source on one side. An average electron dose to the wall was calculated, as was a surface electron dose. Photon dose is correlative results from thermoluminescent dosimeter phantom experiments.

Several publications not included in Table 2 are discussed briefly. Unnikrishnan (*19*) described a bladder model involving a sphere of variable radius. The electron dose rate at the surface of the bladder contents volume (assumed to represent the maximum dose rate) is derived from integration of Berger's scaled absorbed dose distributions (*13*) to represent a spherical volume source. The photon dose is taken directly from the work of Snyder and Ford (*12*). The urine filling rate is constant with an initially empty bladder assumed. Dose to the bladder wall is calculated for ^{131}I-OIH under the assumption of activity entering the bladder either at a constant rate or instantaneously at time zero. The electron and photon dose rates are given as a function of final bladder volume for both sets of assumptions.

Dimitriou et al. (*20*) modified the model of Diffey and Hilson (*16*) for calculation of dose from ^{99m}Tc cystography studies. Here, the bladder volume increases only as a result of saline flow, and all of the activity injected into the catheter is assumed to be in the bladder during the entire filling phase. Complete bladder emptying is assumed. The total dose to the bladder wall is expressed as a function of filling time for a variety of filling rates and for two different delay times between initiation of saline flow and radionuclide injection.

Cloutier et al. (*7*) described a dynamic bladder model that was used for calculating the dose to the fetus from activity in the mother's bladder. Dose to the bladder wall was not calculated. The ellipsoidal bladder is assumed to fill at a constant rate to 300 ml and to be displaced downward as it fills. Monte Carlo calculations are used to select time points at random from the time–activity distribution in the bladder. Because activity is assumed to enter the bladder linearly with time and the volume of the bladder contents also increases linearly with time, this Monte Carlo method weights the calculation according to both activity and bladder size. The activity in the bladder is calculated from the total-body retention function, the excretion rate through the kidney, and the time elapsed since the bladder was emptied. The model provides for voiding intervals of equal or varied time periods. The bladder is assumed to be completely emptied at each void.

Smith et al. (*21*) used the same geometric model and methods for calculating electron and photon dose as Snyder and Ford (*12*). The filling rate is taken as constant with a uniform voiding schedule. Complete emptying is assumed at each void. Radionuclide input is represented by exponential functions with one or more components. Total dose as a function of volume is calculated for 31 radionuclides and fitted with three-component exponential curves. A table of the coefficients for these curves is provided. Dose to the bladder wall is expressed as a function of bladder volume for ^{131}I-OIH and ^{99m}Tc-DTPA. Dose to the bladder wall is shown also as a function of bladder voiding interval for several filling rates and for initial volumes of 0 and 100 ml.

DESCRIPTION OF THE NEW DYNAMIC BLADDER MODEL

The new model incorporates desirable features of the previous methods while introducing innovations that take into consideration some of the complexities of the dynamic situation.

Anatomic Configuration

1. An expanding sphere model was modified from the spherical model of Chen et al. (*4*) that facilitated description by analytical techniques. X-ray images of a contrast-filled bladder demonstrate that the spherical approximation is appropriate for relatively large bladder volumes (*4*). For smaller volumes, the bladder assumes an irregular shape deviating from both the spherical model and the ellipsoidal configuration adopted in some of the previous methods (Table 2). However, as Chen et al. (*4*) point out, the dose to the bladder wall from nonpenetrating radiation (the major fraction of total radiation dose) is relatively independent of the actual bladder shape. Thus, the accuracy of the geometrical description at small volumes is not critical.
2. The volume range for the bladder contents was 10–770 ml. The upper bound of 770 ml results from the dynamic physiologic aspects of the model as listed below, including maximum urine entry rate, initial volume and first voiding time.
3. The wall was characterized to have uniform thinning with bladder contents expansion while maintaining a constant 45-g mass (45 cm^3) (*9,12*).

Physiologic Aspects

1. Variable urine volume entry rates into the bladder [U(t)] corresponded to three different hydration states, consistent with the expected normal daily urine output in the range of 1000–2000 ml: 0.5, 1.0 and 1.5 ml/min. For the 6-hr nighttime gap, the entry rate is reduced to one-half the daytime rate; i.e., 0.25, 0.5 and 0.75 ml/min, respectively.
2. There was a variable activity rate of entry into the bladder [A(t)]). Radiopharmaceuticals were evaluated according to published biologic parameters. Table 3 contains physical and biologic data for the various radiopharmaceuticals. Administration of the radiopharmaceutical was constrained to take place at 9:00 am.
3. The initial bladder-content volume (V_0) range was 10–500 ml.
4. The residual bladder-content volume (V_r) was fixed at 10 ml following each void.
5. Activity was uniformly distributed within the urine.
6. The voiding schedule was as follows: first (initial) voiding time (T_1) was variable from 20 min to 3 hr (evaluation of this parameter for minimum dose is provided for each radiopharmaceutical); 3-hr void intervals following the initial void with a shortened period leading up to midnight, depending on the time available within the 3-hr sequence pattern; and a 6-hr nighttime gap beginning at midnight.

Calculational Methods

1. Radiation dose to the inner surface of the bladder wall was calculated using a modification of the expanding spherical model of Chen et al. (*4*). (Refer to Table 1 for definition of terms.)

   Time-dependent bladder-content volume V(t), with radiopharmaceutical administration taking place at time t = 0, was:

$$V(t) = V_0 + \int U(t)dt: \quad 0 \le t < T_1(1^{st}\text{ void})$$

$$= V_r + \int U(t)dt; \quad T_{n-1} \le t < T_n. \qquad \text{Eq. 1}$$

   Time-dependent bladder contents activity A(t) was:

$$A(t) = A_0 e^{-\lambda t} \sum_{j=1}^{m} \alpha_j (1 - e^{-\lambda_j t})$$

TABLE 3
Physical and Biologic Parameters for the Radiopharmaceuticals Used in the Bladder Wall Dose Calculations

	Physical parameters			Biologic parameters for the bladder contents		
Radiopharmaceutical	Δ_β (mGy · kg/ MBq · sec) (*36*)	Γ' (mGy · cm^2/ MBq · sec)	λ (min^{-1})	Fraction* α_i	Rate constant λ_i (min^{-1})	Reference†
^{18}F-FDG	4.00×10^{-5}	4.13×10^{-4}	6.36×10^{-3}	0.19	3.85×10^{-2}	22
				0.06	1.24×10^{-3}	
^{99m}Tc-DTPA	2.59×10^{-6}	5.63×10^{-5}	1.92×10^{-3}	0.579	1.15×10^{-2}	23
				0.421	1.25×10^{-3}	
^{99m}Tc-pertechnetate	2.59×10^{-6}	5.63×10^{-5}	1.92×10^{-3}	0.328	1.92×10^{-3}	24
				0.306	4.10×10^{-4}	
^{99m}Tc-HEDP	2.59×10^{-6}	5.63×10^{-5}	1.92×10^{-3}	−0.0899	5.42×10^{-2}	25
				0.720	6.47×10^{-3}	
				0.369	6.02×10^{-4}	
^{99m}Tc-MDP	2.59×10^{-6}	5.63×10^{-5}	1.92×10^{-3}	−0.115	5.42×10^{-2}	25
				0.566	1.06×10^{-2}	
				0.549	5.07×10^{-4}	
^{99m}Tc-HMPAO	2.59×10^{-6}	5.63×10^{-5}	1.92×10^{-3}	0.24	1.39×10^{-3}	26
				0.13	2.10×10^{-2}	
^{99m}Tc-glucoheptonate	2.59×10^{-6}	5.63×10^{-5}	1.92×10^{-3}	0.35	3.47×10^{-2}	27
				0.30	4.81×10^{-3}	
				0.35	1.30×10^{-4}	
^{99m}Tc-MAG3	2.59×10^{-6}	5.63×10^{-5}	1.92×10^{-3}	0.51	3.02×10^{-1}	Wooten W.
				0.49	4.05×10^{-2}	*personal communication*
^{99m}Tc-HSA	2.59×10^{-6}	5.63×10^{-5}	1.92×10^{-3}	0.015	1.70×10^{-3}	28
				0.035	3.73×10^{-4}	
				0.95	2.48×10^{-5}	
^{99m}Tc-RBCs	2.59×10^{-6}	5.63×10^{-5}	1.92×10^{-3}	0.90	1.93×10^{-4}	29
				0.0328	1.92×10^{-3}	
				0.0306	4.10×10^{-4}	
^{99m}Tc-MIBI (rest)	2.59×10^{-6}	5.63×10^{-5}	1.92×10^{-3}	0.14	1.65×10^{-3}	30
				0.17	4.81×10^{-4}	
^{99m}Tc-MIBI (stress)	2.59×10^{-6}	5.63×10^{-5}	1.92×10^{-3}	0.10	1.65×10^{-3}	30
				0.20	4.81×10^{-4}	
^{123}I-NaI	4.51×10^{-6}	1.17×10^{-4}	8.75×10^{-4}	0.729	1.90×10^{-3}	31
				0.271	7.41×10^{-6}	
^{131}I-NaI	3.04×10^{-5}	1.61×10^{-4}	5.99×10^{-5}	0.729	1.90×10^{-3}	31
				0.271	7.41×10^{-6}	
^{123}I-OIH	4.51×10^{-6}	1.17×10^{-4}	8.75×10^{-4}	0.51	2.95×10^{-1}	32
				0.49	4.05×10^{-2}	
^{124}I-OIH	3.09×10^{-5}	3.87×10^{-4}	1.15×10^{-4}	0.51	2.95×10^{-1}	32
				0.49	4.05×10^{-2}	
^{131}I-OIH	3.04×10^{-5}	1.61×10^{-4}	5.99×10^{-5}	0.51	2.95×10^{-1}	32
				0.49	4.05×10^{-2}	
^{125}I-iothalamate	3.12×10^{-6}	1.03×10^{-4}	8.00×10^{-6}	0.99	6.92×10^{-3}	33
				0.01	6.88×10^{-5}	
^{111}In-DTPA	5.56×10^{-6}	2.31×10^{-4}	1.70×10^{-4}	0.99	6.92×10^{-3}	34
				0.01	6.88×10^{-5}	
^{89}Sr(SrCl)	9.31×10^{-5}	3.36×10^{-8}	9.53×10^{-6}	0.18	1.93×10^{-3}	35
				0.42	2.41×10^{-4}	

*For radiopharmaceuticals with excretion through the urinary tract only, the coefficients α_i will be the same as those for the total body.
†Reference from which the biologic parameters were taken directly or derived through additional kinetic model analysis (the latter performed by the Radiation Internal Dose Information Center, Oak Ridge, TN).

$$- \sum_{i=1}^{n} [1 - V_r/V(T_i)]A(T_i)e^{-\lambda(t-T_i)}, \quad \text{Eq. 2}$$

where n is the void number (i.e., first void n = 1 and so on). The first term of Equation 2 represents the input into the bladder from the whole body. The expression after the summation sign of the second term represents the activity which leaves the bladder at void time T_i. (The second term is zero before the first void.) Thus, this second term is the sum of administered activity that has been previously voided. Physical decay for each term is included through the exponential function containing the physical decay constant.

Dose per unit administered activity to the bladder wall inner surface was:

$$\bar{D}/A_0 = (1/A_0)\int_0^\infty [3.9\Gamma' A(t)/V(t)^{2/3} + \Delta_\beta A(t)/(2\rho V(t))]dt. \quad \text{Eq. 3}$$

TABLE 4
Percentile Distance within which 50% (x_{50}) and 90% (x_{90}) of the Electron Energy is Absorbed in the Bladder Wall (Soft Tissue) (*13*)*
For comparison, the bladder wall thickness as a function of bladder-contents volume for the new model is provided below.

Radionuclide	x_{50} (cm)	x_{90} (cm)
^{18}F	0.038	0.0939
^{99m}Tc	0.0090	0.0148
^{123}I	0.0093	0.0166
^{124}I	0.182	0.431
^{131}I	0.0285	0.0822

*Values for ^{18}F, ^{124}I, and ^{131}I are taken directly from reference 13. Values for ^{99m}Tc and ^{123}I are derived from results of Reference 13 for monoenergetic electrons and known abundances of the emissions of these nuclides.

	Bladder contents volume (cm^3)				
	50	100	300	500	800
Bladder wall thickness (cm†)	0.55	0.38	0.20	0.14	0.11

†Spherical-shell bladder-wall volume remains constant at 45 cm^3.

Considerations leading to this analytic expression as derived by Chen et al. (*4*) were described earlier in the text and in Table 2 as Model D. The calculations as performed by numerical integration were terminated when the ratio of the dose in a given interval between voids to the total dose including that interval was < 0.001%, i.e., $D(n \rightarrow n + 1)/D(1 \rightarrow n + 1) \leq 10^{-5}$.

2. Electron dose at depth into the bladder wall was determined as follows. Depth dose characteristics for point sources or discrete distributions of radionuclides may be described through use of the percentile distance parameter, which denotes the fraction of emitted energy absorbed in a sphere of radius x around the source. Thus, x_{90} and x_{50} specify the distance from the source within which 90% and 50%, respectively, of the energy is absorbed. The values of these parameters, as given by Berger (*13*), for some of the radionuclides evaluated in this report, are given in Table 4. For beta emitters, the values are taken directly from a previous report (*13*). For nuclides with a series of electron emissions, the percentile distance values are determined through consideration of the energies and abundances of the various emissions and the values given (*13*) for the individual energies. Formulas for extension of these solutions for point sources to the spherical volume source geometry assumed for the bladder are taken from a previous report (*14*). Bladder size is determined at each time step by solution of the time-dependent bladder-content volume expression (Eq. 1) using the optimal first void time (as determined by average bladder-wall dose) and three different values of initial volume. Integration of the final expression is accomplished by use of the trapezoidal integration method.

RESULTS

A variety of commonly used radiopharmaceuticals was studied to provide a comparison among bladder wall dosimetry models and to evaluate the new model. These include: ^{18}F-FDG

TABLE 5
Comparison of the Absorbed Dose per Unit Administered Activity at the Bladder Wall Surface for the Various Models for Selected Radiopharmaceuticals

	Bladder model												
	Initial volume	Model A MIRD 5 (Revised) (*5*)		Model B Snyder and Ford (*12*)		Model C Diffey and Hilson (*16*)		Model D Chen et al. (*4*)		This report (1.0/0.5 ml/min)	
Radionuclide	V_0 (ml)	T_{1m}* (min)	$\bar{D}/A_0$ (mGy/MBq)	T_{1m}* (min)	$\bar{D}/A_0$ (mGy/MBq)	T_{1m}* (min)	$\bar{D}/A_0$ (mGy/MBq)	T_{1m}* (min)	$\bar{D}/A_0$ (mGy/MBq)	T_{1m}* (min)	$\bar{D}/A_0$ (mGy/MBq)
^{18}F-FDG	10	—	—	40	0.22	40	0.20	40	0.23	40	0.31
	200	40	0.059	60	0.081	80	0.065	60–80	0.084	80	0.091
	500	—	—	80	0.049	100	0.038	80–100	0.051	100	0.053
^{99m}Tc-DTPA	10	—	—	60–80	0.076	60–80	0.077	60–80	0.083	80	0.099
	200	60	0.029	120–140	0.048	140	0.045	120–140	0.050	160	0.055
	500	—	—	140–180	0.035	160–180	0.033	160–180	0.037	180+	0.041
^{99m}Tc-MAG3	10	—	—	20	0.11	20	0.12	20	0.12	40	0.19
	200	20	0.032	40	0.046	40–60	0.046	40	0.049	60	0.051
	500	—	—	60	0.030	40–80	0.030	60	0.032	60	0.030
^{131}I-NaI	10	—	—	180+	0.81	180+	0.81	180+	0.86	120	0.93
	200	180+	0.46	180+	0.78	180+	0.78	180+	0.84	180+	0.78
	500	—	—	180+	0.76	180+	0.76	180+	0.81	180+	0.74
^{123}I-OIH	10	—	—	20	0.18	20	0.18	20	0.25	40	0.38
	200	20–40	0.065	40	0.073	40–60	0.070	40	0.10	60	0.10
	500	—	—	60	0.046	60	0.043	60	0.068	60	0.061
^{124}I-OIH	10	—	—	20	1.20	20	1.30	20	1.40	40	2.15
	200	20–40	0.43	40–60	0.49	40–60	0.49	40	0.57	60	0.56
	500	—	—	60	0.30	60	0.30	40–80	0.41	80	0.32
^{131}I-OIH	10	—	—	20	1.00	20	1.02	20	1.20	40	1.82
	200	20–40	0.30	60	0.35	60	0.35	40–60	0.43	60	0.45
	500	—	—	60	0.22	60	0.22	60–80	0.27	80	0.25

*T_{1m} represents the initial (first) void time which provides minimum dose for the given initial volume V_0.
Explanatory points for T_{1m}: (a) a value of 40–80 indicates that the same minimum dose value as shown in the adjacent column was obtained for initial void times of 40, 60, 80 min; (b) a value of 140–180 indicates that the same minimum dose value was obtained for initial void times from 140 out to 180 min; and (c) a value of 180+ indicates that the minimum dose value calculated occurred at the 180-min void point and is that value shown in the adjacent column. The actual dose minimum may occur at longer initial void times.

TABLE 6
Electron Depth: Dose per Unit Administered Activity to the Bladder Wall at the Surface, x_{50} and x_{90}

Radiopharmaceutical	Initial volume V_0 (ml)	Bladder fill rate U(t) (ml/min)	Time of first void T_1 (min)	Absorbed dose/administered activity (mGy/MBq)		
				Surface	At x_{50}	At x_{90}
^{18}F-FDG	10	0.5	40	4.4E-01	8.7E-02	7.3E-03
	10	1.0	40	2.5E-01	4.8E-02	4.1E-03
	10	1.5	40	1.7E-01	3.4E-02	2.9E-03
	200	0.5	80	8.6E-02	1.7E-02	1.5E-03
	200	1.0	80	6.3E-02	1.3E-02	1.1E-03
	200	1.5	80	5.3E-02	1.1E-02	9.1E-04
	500	0.5	100	4.5E-02	9.2E-03	7.8E-04
	500	1.0	100	3.5E-02	7.0E-03	6.0E-04
	500	1.5	100	3.0E-02	6.0E-03	5.1E-04
^{99m}Tc-DTPA	10	0.5	80	1.1E-01	1.8E-02	1.4E-03
	10	1.0	80	5.9E-02	9.1E-03	7.1E-04
	10	1.5	80	4.0E-02	6.1E-03	4.8E-04
	200	0.5	160	4.6E-02	1.6E-02	1.2E-03
	200	1.0	160	2.9E-02	8.1E-03	6.3E-04
	200	1.5	160	2.2E-02	5.4E-03	4.2E-04
	500	0.5	180	3.3E-02	5.0E-03	3.9E-04
	500	1.0	180	2.1E-02	3.1E-03	2.4E-04
	500	1.5	180	1.6E-02	2.3E-03	1.8E-04
^{99m}Tc-pertechnetate	10	0.5	100	3.4E-02	5.7E-03	4.6E-04
	10	1.0	100	1.8E-02	3.0E-03	2.2E-04
	10	1.5	100	1.2E-02	1.9E-03	1.5E-04
	200	0.5	180	2.2E-02	3.2E-03	2.6E-04
	200	1.0	180	1.2E-02	1.9E-03	1.5E-04
	200	1.5	180	8.8E-03	1.3E-03	1.0E-04
	500	0.5	180	2.0E-02	3.0E-03	2.4E-04
	500	1.0	180	1.1E-02	1.7E-03	1.3E-04
	500	1.5	180	7.8E-03	1.2E-03	9.2E-05
^{99m}Tc-HEDP	10	0.5	120	8.4E-02	2.7E-02	2.2E-03
	10	1.0	120	4.3E-02	1.5E-02	1.2E-03
	10	1.5	120	2.9E-02	1.1E-02	8.4E-04
	200	0.5	180	4.3E-02	1.7E-02	1.4E-03
	200	1.0	180	2.6E-02	1.1E-02	8.6E-04
	200	1.5	180	1.9E-02	8.1E-03	6.5E-04
	500	0.5	180	3.6E-02	1.6E-02	1.3E-03
	500	1.0	180	2.1E-02	1.0E-02	7.8E-04
	500	1.5	180	1.5E-02	7.6E-03	5.9E-04
^{99m}Tc-MDP	10	0.5	120	7.5E-02	3.0E-02	2.3E-03
	10	1.0	120	3.8E-02	1.7E-02	1.3E-03
	10	1.5	120	2.6E-02	1.2E-02	9.5E-04
	200	0.5	180	3.5E-02	1.9E-02	1.5E-03
	200	1.0	180	2.1E-02	1.2E-02	9.6E-04
	200	1.5	180	1.6E-02	9.3E-03	7.3E-04
	500	0.5	180	2.7E-02	1.8E-02	1.4E-03
	500	1.0	180	1.6E-02	1.1E-02	8.9E-04
	500	1.5	180	1.2E-02	8.7E-03	6.8E-04
^{99m}Tc-HMPAO	10	0.5	80	3.8E-02	5.9E-03	4.6E-04
	10	1.0	80	2.0E-02	3.0E-03	2.4E-04
	10	1.5	80	1.4E-02	2.1E-03	1.6E-04
	200	0.5	120	1.7E-02	3.8E-03	3.0E-04
	200	1.0	120	1.0E-02	1.9E-03	1.5E-04
	200	1.5	120	7.6E-03	1.3E-03	1.1E-04
	500	0.5	180	1.3E-02	1.9E-03	1.5E-04
	500	1.0	180	7.5E-03	1.1E-03	8.9E-05
	500	1.5	180	5.7E-03	8.4E-04	6.5E-05
^{99m}Tc-glucoheptonate	10	0.5	60	1.1E-01	1.6E-02	1.2E-03
	10	1.0	60	5.5E-02	8.2E-03	6.4E-04
	10	1.5	60	3.8E-02	5.6E-03	4.3E-04
	200	0.5	100	3.8E-02	7.3E-03	5.7E-04
	200	1.0	100	2.3E-02	4.0E-03	3.1E-04
	200	1.5	100	1.8E-02	2.9E-03	2.3E-04
	500	0.5	140	2.5E-02	8.0E-03	6.3E-04
	500	1.0	140	1.6E-02	4.0E-03	3.1E-04
	500	1.5	140	1.2E-02	2.7E-03	2.1E-04

TABLE 6
Continued

Radiopharmaceutical	Initial volume V_0 (ml)	Bladder fill rate U(t) (ml/min)	Time of first void T_1 (min)	Absorbed dose/administered activity (mGy/MBq)		
				Surface	At x_{50}	At x_{90}
^{99m}Tc-MAG	10	0.5	40	2.3E-01	3.2E-02	2.5E-03
	10	1.0	40	1.2E-01	1.8E-02	1.4E-03
	10	1.5	40	8.7E-02	1.2E-02	9.7E-04
	200	0.5	60	3.8E-02	7.3E-03	5.7E-04
	200	1.0	60	2.7E-02	4.6E-03	3.5E-04
	200	1.5	60	2.3E-02	3.4E-03	2.7E-04
	500	0.5	60	2.2E-02	4.5E-03	3.5E-04
	500	1.0	60	1.5E-02	2.6E-03	2.0E-04
	500	1.5	60	1.2E-02	2.0E-03	1.6E-04
^{99m}Tc-HSA	10	0.5	120	3.8E-03	7.0E-04	5.4E-05
	10	1.0	120	2.0E-03	3.2E-04	2.7E-05
	10	1.5	120	1.4E-03	2.3E-04	1.8E-05
	200	0.5	180	2.9E-03	4.3E-04	3.5E-05
	200	1.0	180	1.6E-03	2.4E-04	1.9E-05
	200	1.5	180	1.1E-03	1.7E-04	1.3E-05
	500	0.5	180	2.7E-03	4.3E-04	3.2E-05
	500	1.0	180	1.4E-03	2.2E-04	1.7E-05
	500	1.5	180	1.0E-03	1.5E-04	1.2E-05
^{99m}Tc-RBCs	10	0.5	100	1.6E-02	2.7E-03	2.2E-04
	10	1.0	100	8.3E-03	1.4E-03	1.1E-04
	10	1.5	100	5.6E-03	9.2E-04	7.0E-05
	200	0.5	180	1.2E-02	1.9E-03	1.5E-04
	200	1.0	180	6.5E-03	1.0E-03	7.8E-05
	200	1.5	180	4.6E-03	7.0E-04	5.4E-05
	500	0.5	180	1.1E-02	1.8E-03	1.4E-04
	500	1.0	180	6.1E-03	9.5E-04	7.3E-05
	500	1.5	180	4.2E-03	6.5E-04	5.1E-05
^{99m}Tc-MIBI (rest)	10	0.5	100	1.5E-02	2.6E-03	2.1E-04
	10	1.0	100	7.9E-03	1.3E-03	1.0E-04
	10	1.5	100	5.4E-03	8.6E-04	6.8E-05
	200	0.5	180	1.0E-02	1.6E-03	1.2E-04
	200	1.0	180	5.8E-03	8.6E-04	6.8E-05
	200	1.5	180	4.1E-03	6.2E-04	4.9E-05
	500	0.5	180	9.6E-03	1.5E-03	1.2E-04
	500	1.0	180	5.2E-03	7.8E-04	6.2E-05
	500	1.5	180	3.6E-03	5.4E-04	4.3E-05
^{99m}Tc-MIBI (stress)	10	0.5	100	1.3E-02	2.3E-03	1.8E-04
	10	1.0	100	6.9E-03	1.1E-03	1.0E-04
	10	1.5	100	4.7E-03	7.6E-04	5.9E-05
	200	0.5	180	9.2E-03	1.4E-03	1.1E-04
	200	1.0	180	5.1E-03	7.8E-04	5.9E-05
	200	1.5	180	3.6E-03	5.4E-04	4.3E-05
	500	0.5	180	8.5E-03	1.3E-03	1.0E-04
	500	1.0	180	4.6E-03	7.0E-04	5.4E-05
	500	1.5	180	3.2E-03	4.9E-04	3.8E-05
^{123}I-NaI	10	0.5	100	1.5E-01	3.1E-02	2.7E-03
	10	1.0	100	7.5E-02	1.5E-02	1.3E-03
	10	1.5	100	5.0E-02	9.5E-03	8.6E-04
	200	0.5	180	1.1E-01	1.8E-02	1.6E-03
	200	1.0	180	5.7E-02	9.5E-03	8.6E-04
	200	1.5	180	4.0E-02	6.8E-03	5.9E-04
	500	0.5	180	9.8E-02	1.7E-02	1.5E-03
	500	1.0	180	5.2E-02	8.9E-03	7.8E-04
	500	1.5	180	3.6E-02	6.2E-03	5.4E-04
^{131}I-NaI	10	0.5	120	1.6E-00	3.0E-01	2.4E-02
	10	1.0	120	7.9E-01	1.5E-01	1.2E-02
	10	1.5	120	5.3E-01	1.0E-01	8.1E-03
	200	0.5	180	1.3E-00	3.0E-01	2.4E-02
	200	1.0	180	6.6E-01	1.6E-01	1.2E-02
	200	1.5	180	4.5E-01	1.1E-01	8.6E-03
	500	0.5	180	1.2E-00	3.0E-01	2.3E-02
	500	1.0	180	6.2E-01	1.5E-01	1.2E-02
	500	1.5	180	4.3E-01	1.0E-01	8.1E-03

TABLE 6
Continued

Radiopharmaceutical	Initial volume V_0 (ml)	Bladder fill rate U(t) (ml/min)	Time of first void T_1 (min)	Absorbed dose/administered activity (mGy/MBq)		
				Surface	At x_{50}	At x_{90}
^{123}I-OIH	10	0.5	40	4.2E-01	6.5E-02	5.7E-03
	10	1.0	40	2.3E-01	3.5E-02	3.2E-03
	10	1.5	40	1.6E-01	2.5E-02	2.2E-03
	200	0.5	60	7.3E-02	1.2E-02	1.1E-03
	200	1.0	60	5.1E-02	8.1E-03	7.3E-04
	200	1.5	60	4.2E-02	6.6E-03	5.9E-04
	500	0.5	60	4.2E-02	7.3E-03	6.5E-04
	500	1.0	60	2.9E-02	4.6E-03	4.1E-04
	500	1.5	60	2.3E-02	3.7E-03	3.2E-04
^{124}I-OIH	10	0.5	40	3.1E-00	4.6E-01	2.0E-02
	10	1.0	40	1.6E-00	2.5E-01	1.1E-02
	10	1.5	40	1.1E-00	1.7E-01	7.6E-03
	200	0.5	60	5.4E-01	8.9E-02	4.0E-03
	200	1.0	60	3.7E-01	6.0E-02	2.7E-03
	200	1.5	60	3.0E-01	4.9E-02	2.2E-03
	500	0.5	80	2.7E-01	4.9E-02	2.2E-03
	500	1.0	80	2.0E-01	3.2E-02	1.5E-03
	500	1.5	80	1.7E-01	2.7E-02	1.3E-03
^{131}I-OIH	10	0.5	40	3.0E-00	6.5E-01	5.1E-02
	10	1.0	40	1.6E-00	3.5E-01	2.7E-02
	10	1.5	40	1.1E-00	2.4E-01	1.9E-02
	200	0.5	60	5.4E-01	1.2E-01	1.0E-02
	200	1.0	60	3.7E-01	8.4E-02	6.5E-03
	200	1.5	60	3.0E-01	6.8E-02	5.4E-03
	500	0.5	80	2.7E-01	6.8E-02	5.4E-03
	500	1.0	80	2.0E-01	4.3E-02	3.5E-03
	500	1.5	80	1.7E-01	3.8E-02	3.0E-03

(*22*), ^{99m}Tc-DTPA (*23*), ^{99m}Tc-pertechnetate (*24*), ^{99m}Tc-HEDP (*25*), ^{99m}Tc-MDP (*25*), ^{99m}Tc-HMPAO (*26*), ^{99m}Tc-glucoheptonate (*27*), ^{99m}Tc-MAG3 (Wooten W, St. Agnes Medical Center, Fresno, CA, *personal communication*), ^{99m}Tc-HSA (*28*), ^{99m}Tc-RBCs (*29*), ^{99m}Tc-sestamibi (rest and stress) (*30*), ^{123}I-NaI (*31*), ^{131}I-NaI (*31*), ^{123}I-OIH (*32*), ^{124}I-OIH (*32*), ^{131}I-OIH (*32*), ^{125}I-iothalamate (*33*), ^{111}In-DTPA (*34*) and ^{89}Sr-SrCl (*35*). The biological parameters for these radiopharmaceuticals were taken or derived from the references cited (Table 3).

The radiation absorbed dose per unit administered activity $\bar{D}/A_0$ to the inner bladder wall surface was calculated for each radiopharmaceutical as a function of initial bladder contents volume (V_0) and first void time (T_1). As a function of these parameters, families of dose curves as well as tabular data were generated for each model. For the previously published models (Table 2), 3-hr voiding intervals were assumed after the variable first void time. In the Appendix, Figures A1–A4 provide examples of the ^{99m}Tc-DTPA results for these models with the calculations presented in Tables A1–A4.

Similar calculations for the new model are shown in Figures A5–A24 and are presented in Tables A5–A24. For the figures, only the results for a bladder urine input function U(t) = 1.0/0.5 ml/min (day/night) are shown. The tables provide data for the other entry rates evaluated (i.e., 0.5/0.25 and 1.5/0.75 ml/min). Examples of the bladder activity curves for two radiopharmaceuticals are shown in Figures A25 and A26 for U(t) = 1.0/0.5 ml/min, V_0 = 100 ml and T_1 = 60 min.

A comparison of the absorbed dose per unit administered activity at the bladder wall inner surface is contained in Table 5 for all models for selected radiopharmaceuticals. Values are given for the initial void time which results in minimum dose (T_{1m}) for the initial bladder volume specified.

Table 6 provides the electron absorbed dose per unit administered activity at the bladder wall surface and at the distances x_{50} and x_{90} as calculated by the new model for selected radiopharmaceuticals for three different V_0 and U(t) values. The first void times represent the optimal first void time (T_{1m} as determined by the surface dose evaluation) or a value close to that. Figures A27 and A28 show examples of the electron dose per unit administered activity as a function of distance into the bladder wall for ^{18}F FDG and ^{99m}Tc-DTPA under selected conditions.

DISCUSSION AND CONCLUSION

The published models for urinary bladder wall dose have provided a useful framework for development of the new comprehensive dynamic bladder model. Provisions for an expanding/contracting bladder with variable initial volume, first void time and rate of urine entry, along with options for residual volume allow a more detailed understanding of bladder wall dosimetry than offered by the MIRD 5 (Revised) model.

Inspection of the comparative results in Table 5 for selected radiopharmaceuticals indicates that the new model tends to give the highest dose to the bladder wall surface; however, the results are essentially similar to those provided by the model of Chen et al. (*4*) (Model D). When compared with the MIRD 5 (Revised) (Model A) for an initial volume of 200 ml, values for the new model are approximately 57% higher (range 30%–83% higher). The Snyder and Ford (*12*) (Model B) and Diffey and Hilson (*16*) (Model C) models provide roughly identical results for dose to the bladder wall that are, in general, slightly less than those given by the new model.

Each radiopharmaceutical has a unique time–activity curve for bladder activity. This variability, when combined with a nonuniform voiding schedule and analyzed in terms of initial bladder volume and first bladder voiding time, may be used to predict the optimum first voiding time and most desirable hydration states. Large initial bladder volumes and higher rates of urine flow into the bladder result in lower total bladder wall dose. Earlier first voiding times do not necessarily result in lower total bladder wall doses. In fact, the results indicate that the optimum first voiding time is from 40 min to 3 hr after administration, depending on the radiopharmaceutical. The optimum first void time (T_{1m}) does not appear to be sensitive to the model used.

Electron dose decreases rapidly with increasing depth in the wall at a gradient determined by the electron energy spectrum. For most nuclear medicine radiopharmaceuticals, 90% of the energy is deposited within 0.1 cm of the bladder interior wall surface. An exception is ^{124}I, potentially a contaminant in ^{123}I. Other high-energy beta emitters such as ^{90}Y or other therapy agents, however, might contribute a significant dose deep into the bladder wall and possibly even into surrounding tissues.

ACKNOWLEDGMENTS

We gratefully acknowledge the assistance of William S. Kassing in preparing the figures and tables for this revised Pamphlet.

REFERENCES

1. Thomas SR, Stabin MG, Chen C-T, Samaratunga RC. MIRD Pamphlet No. 14: a Dynamic Urinary Bladder Model for Radiation Dose, Calculations. *J Nucl Med* 1992;33:783–802.
2. [Erratum]. *J Nucl Med* 1994;35:73.
3. Dowd MT, Chen C-T, Wendel MJ, Faulhaber PJ, Cooper MD. Radiation dose to the bladder wall from 2-^{18}F]fluoro-2-deoxy-D-glucose in adult humans. *J Nucl Med* 1991;32:707–712.
4. Chen C-T, Harper PV, Lathrop KA. A simple dynamic model for calculating radiation absorbed dose to the bladder wall. In: Schlafke-Stelson AT, Watson EE, eds. *Fourth International Radiopharmaceutical Dosimetry Symposium*, Nov. 5–8, 1985, Oak Ridge, TN: CONF-851113-(DE86010102), 587–612.
5. Snyder WS, Ford MR, Warner GG. MIRD Pamphlet No. 5 (Revised): estimates of specific absorbed fractions for photon sources uniformly distributed in various organs of heterogeneous phantom. New York: The Society of Nuclear Medicine: 1978.
6. Cristy M, Eckerman KF. *Specific absorbed fractions of energy at various ages from internal photon sources. I. Methods*, ORNL Publ. No. TM-8381/V1. 1987.
7. Cloutier RJ, Smith SA, Watson EE, et al. Dose to the fetus from radionuclides in the bladder. *Health Phys* 1973;25:147–161.
8. Loevinger R, Budinger TF, Watson EE. MIRD primer for absorbed dose calculations. New York: The Society of Nuclear Medicine; 1988.
9. Snyder WS, Ford MR, Warner GG, Watson SB. MIRD Pamphlet No. 11: "S," absorbed dose per unit cumulated activity for selected radionuclides and organs. New York: The Society of Nuclear Medicine: 1975.
10. Snyder WS, Ford MR, Warner GG, Watson SB. A tabulation of dose equivalent per microcurieday for source and target organs of an adult for various radionuclides. ORNL 5000. Oak Ridge TN: Oak Ridge National Laboratory; 1975.
11. Loevinger R, Japha EM, Brownell GL. Discrete radioisotope sources. In: Hine GJ, Brownell GL, eds. *Radiation dosimetry*. New York: Academic Press; 1956:693–799.
12. Snyder WS, Ford MR. Estimation of dose to the urinary bladder and to the gonads. In: Cloutier RJ, Coffey JL, Snyder WS, Watson EE, eds. *Radiopharmaceutical dosimetry symposium*, HEW Publication (FDA) 76-8044, 1976. Oak Ridge, TN, April 26–29, 1976. 313–350.
13. Berger MJ. MIRD Pamphlet No. 7: distribution of absorbed dose around point sources of electrons and beta particles in water and other media. *J Nucl Med* 1971;12(supp 5).
14. Berger MJ. *Beta-ray dosimetry calculations with the use of point kernels in medical radionuclides, radiation dose and effects*, AEC Symposium Series No. 20. USAEC Division of Technical Information, 1970.
15. Smith EM, Warner GG. Practical methods of dose reduction to the bladder wall. In: *Radiopharmaceutical dosimetry symposium*. Oak Ridge, TN, April 26–29, 1976. 351–359.
16. Diffey B, Hilson A. Absorbed dose to the bladder form. ^{99m}Tc-DTPA [Letter]. *Br J Radiol* 1976;49:196–198.
17. Powell GR, Chen C-T. Radiation absorbed dose to bladder walls from positron emitters in the bladder content. *Med Phys* 1987;14:1079–1086.
18. Bochkarev VV, Radzievsky GB, Timofeev LV, Demiano DA. Distribution and absorbed energy from a point beta-source in a tissue equivalent medium. *Int J Appl Radiat Isot* 1972;23:493.
19. Unnikrishnan K. Dose to the urinary bladder from radionuclides in urine. *Phys Med Biol* 1974;19:329–340.
20. Dimitriou P, Fretzayas A, Nicolaidou P, et al. Estimates of dose to the bladder during direct radionuclide cystography: concise communication. *J Nucl Med* 1984;25:792–795.
21. Smith T, Veall N, Wotton R. Bladder wall dose from administered radiopharmaceuticals: the effects of variations in urine flow rate, voiding interval, and initial bladder content. *Radiat Prot Dosim* 1982;2:183–189.
22. Jones S, Alavi A, Christman D, Montanez I, Wolf A, Reivich M. The radiation dosimetry of 2-[F-18]fluoro-2-deoxy-D-glucose in man. *J Nucl Med* 1982;23:613–617.
23. Thomas SR, Atkins HL, McAfee JG, et al. MIRD Dose Estimate Report No. 12: radiation absorbed dose from Tc-99m diethylenetriaminepentaacetic acid (DTPA). *J Nucl Med* 1984;25:503–505.
24. Lathrop KA, Atkins HL, Berman M, et al. Summary of current radiation dose estimates to normal humans from Tc-99m as sodium pertechnetate. *J Nucl Med* 1976;17:74–77.
25. Weber DA, Makler PT Jr, Watson EE, et al. Radiation absorbed dose from technetium-99-labeled bone imaging agents. *J Nucl Med* 1989;30:1117–1122.
26. Soundy RG, Tyrell DA, Pickett RD, Stabin MG. The radiation dosimetry of Tc- 99m exametazime. *Nucl Med Commun* 1990;11:791–799.
27. Radiation dose to patients from radiopharmaceuticals (technetium-gluconate, glucoheptonate). In: ICRP Publication No. 53. a report of Task Group of Committee 2 of the International Commission on Radiation Protection. Elmsford, NY: Pergamon Press, Inc.; 1988:193–194.
28. Radiation dose to patients from radiopharmaceuticals (technetium-labelled albumin (HSA)). In: ICRP Publication No. 53: a report of Task Group of Committee 2 of the International Commission on Radiation Protection. Elmsford, NY: Pergamon Press, Inc.; 1988:173.
29. Radiation dose to patients from radiopharmaceuticals (technetium-labelled erythrocytes). In: ICRP Publication No. 53: a report of Task Group of Committee 2 of the International Commission on Radiation Protection. Elmsford, NY: Pergamon Press, Inc.; 1988:209–210.
30. Radiation dose to patients from radiopharmaceuticals (technetium-labelled MIBI). In: ICRP Publication No. 62: a report of Task Group of Committee 2 of the International Commission on Radiation Protection. Tarrytown, NY: Pergamon Press, Inc.; 1993: 21–24.
31. Berman M, Braverman LE, Burke J, et al, Summary of current radiation dose estimates to humans from I-123, I-124, I-125, I-126, I-130, I-131, and I-132 as sodium iodide. *J Nucl Med* 1975;16:857–860.
32. Lindmo T, Skeretting A, Nakken K. An examination of different mathematical models for renal function as measured by ^{131}I-hippuran renography. *Med Phys* 1974;1:193–197.
33. Radiation dose to patients from radiopharmaceuticals (iothalamate). In: ICRP Publication No. 53: a report of Task Group of Committee 2 of the International Commission on Radiation Protection. Elmsford, NY: Pergamon Press, Inc.; 1988:315–316.
34. Radiation dose to patients from radiopharmaceuticals (indium-DTPA). In: ICRP Publication No. 53: a report of Task Group of Committee 2 of the International Commission on Radiation Protection. Elmsford, NY: Pergamon Press, Inc.; 1988:237–240.
35. Radiation dose to patients form radiopharmaceuticals (strontium). In: ICRP Publication No. 53: a report of Task Group of Committee 2 of the International Commission on Radiation Protection. Elmsford, NY: Pergamon Press, Inc.; 1988:169–171.
36. Weber DA, Eckerman KF, Dillman LT, et al. *MIRD: radionuclide data and decay schemes*. New York: The Society of Nuclear Medicine; 1989.

APPENDIX A

DTPA calculations for the various models are shown in Figures A1–A4 and Tables A1–A4. Calculations for the new model are shown in Figures A5-A24 and Tables A5–A24.

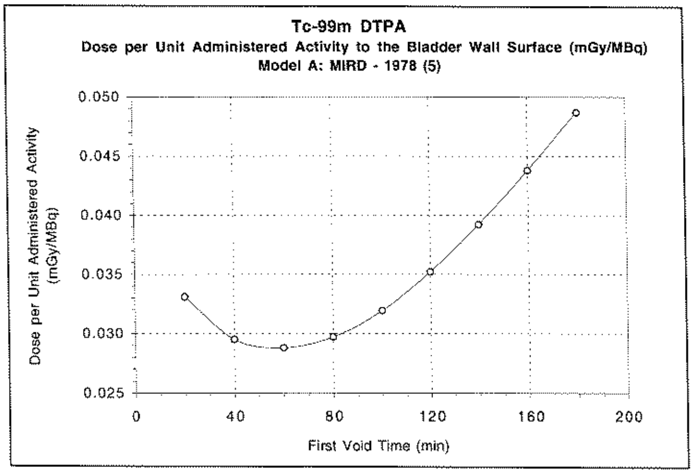

FIGURE A1. Model A [MIRD Pamplet No. 5 Revised (5)], ^{99m}Tc-DTPA. Dose per unit administered activity to the urinary bladder wall surface as a function of first void time (T_1) (constant volume). Urine entry rate U(t) = 1.25 ml/min (constant at all times). Voiding schedule = every 3 hr after initial void, 10 voids total included in the dose calculation and no nighttime gap.

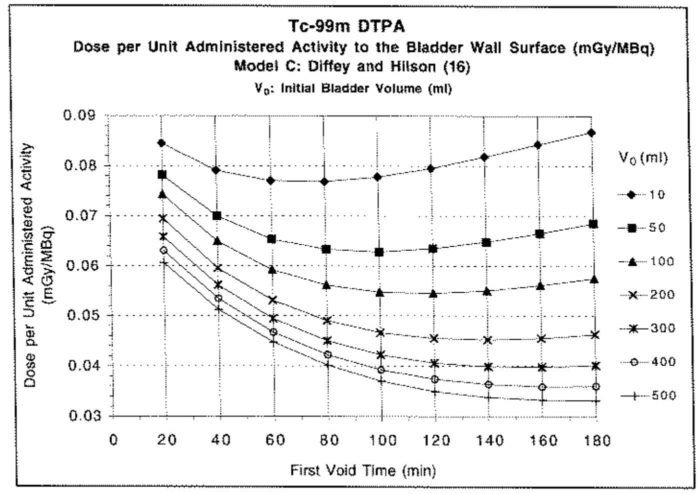

FIGURE A3. Model C [Diffey and Hilson (*16*)], ^{99m}Tc-DTPA. Dose per unit administered activity to the urinary bladder wall surface as a function of first void time (T_1) for various values of initial bladder contents (V_0). Urine entry rate U(t) and voiding schedule were the same as those in Figure A1.

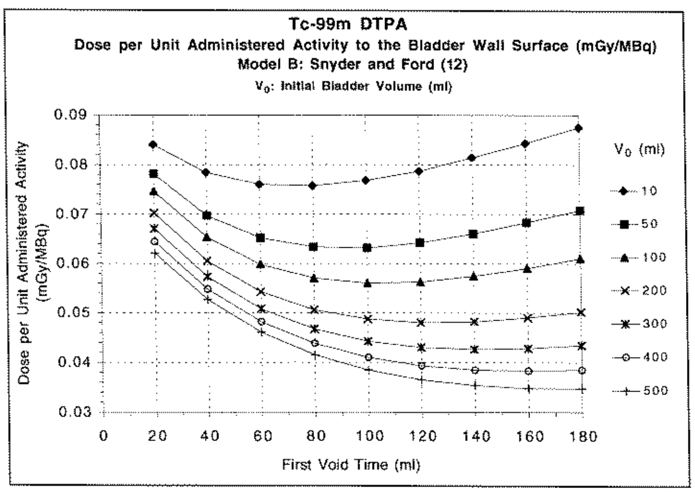

FIGURE A2. Model B [Snyder and Ford (*12*)], ^{99m}Tc-DTPA. Dose per unit administered activity to the urinary bladder wall surface as a function of first void time (T_1) for various values of initial bladder contents (V_0). Urine entry rate U(t) and voiding schedule were the same as those in Figure A1.

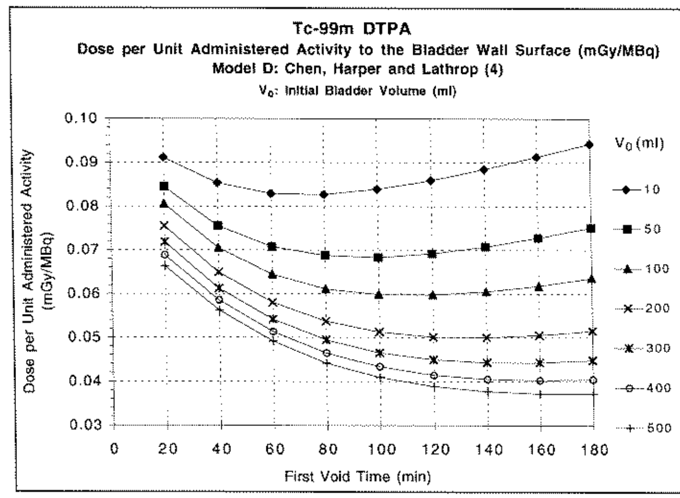

FIGURE A4. Model D [Chen et al. (*4*)], ^{99m}Tc-DTPA. Dose per unit administered activity to the urinary bladder wall surface as a function of first void time (T_1) for various values of initial bladder contents (V_0). Urine entry rate U(t) and voiding schedule were the same as those in Figure A1.

TABLE A1
Technetium-99m-DTPA Dose per Unit Administered Activity to the Bladder Wall Surface (mGy/MBq) Model A: MIRD, 1978 (5)

First void time (min)								
20	40	60	80	100	120	140	160	180
0.033	0.030	0.029	0.030	0.032	0.035	0.039	0.044	0.049

TABLE A2
Technetium-99m-DTPA Dose per Unit Administered Activity to the Bladder Wall Surface (mGy/MBq)
Model B: Snyder and Ford (*12*)

	First void time (min)								
V_0 (ml)	20	40	60	80	100	120	140	160	180
10	0.084	0.078	0.076	0.076	0.077	0.079	0.081	0.084	0.088
50	0.078	0.070	0.065	0.063	0.063	0.064	0.066	0.068	0.071
100	0.075	0.065	0.060	0.057	0.056	0.056	0.057	0.059	0.061
200	0.070	0.061	0.054	0.051	0.049	0.048	0.048	0.049	0.050
500	0.062	0.053	0.046	0.042	0.038	0.037	0.035	0.035	0.035

V_0 = initial Bladder Volume (ml).

TABLE A3
Technetium-99m-DTPA Dose per Unit Administered Activity to the Bladder Wall Surface (mGy/MBq)
Model C: Diffey and Hilson (*16*)

	First void time (min)								
V_0 (ml)	20	40	60	80	100	120	140	160	180
10	0.085	0.079	0.077	0.077	0.078	0.080	0.082	0.084	0.087
50	0.078	0.070	0.065	0.063	0.063	0.064	0.065	0.067	0.069
100	0.074	0.065	0.059	0.056	0.055	0.055	0.055	0.056	0.058
200	0.069	0.060	0.053	0.049	0.047	0.046	0.045	0.046	0.046
500	0.061	0.051	0.045	0.040	0.037	0.035	0.034	0.033	0.033

V_0 = initial bladder volume (ml).

TABLE A4
Technetium-99m-DTPA Dose per Unit Administered Activity to the Bladder Wall Surface (mGy/MBq)
Model D: Chen et al. (*4*)

	First void time (min)								
V_0 (ml)	20	40	60	80	100	120	140	160	180
10	0.091	0.085	0.083	0.083	0.084	0.086	0.089	0.091	0.094
50	0.085	0.076	0.071	0.069	0.068	0.069	0.071	0.073	0.075
100	0.081	0.071	0.064	0.061	0.060	0.060	0.061	0.062	0.064
200	0.076	0.065	0.058	0.054	0.051	0.050	0.050	0.051	0.052
500	0.066	0.056	0.049	0.044	0.041	0.039	0.038	0.037	0.037

V_0 = initial bladder volume (ml).

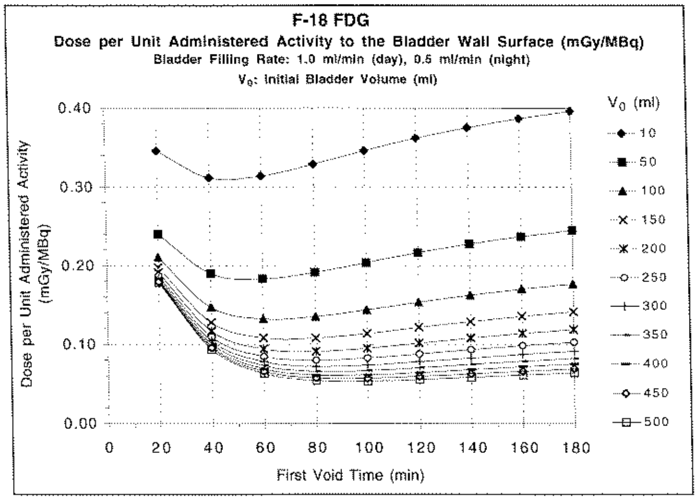

FIGURE A5. New model for ^{18}F-FDG. Dose per unit administered activity to the urinary bladder wall surface.

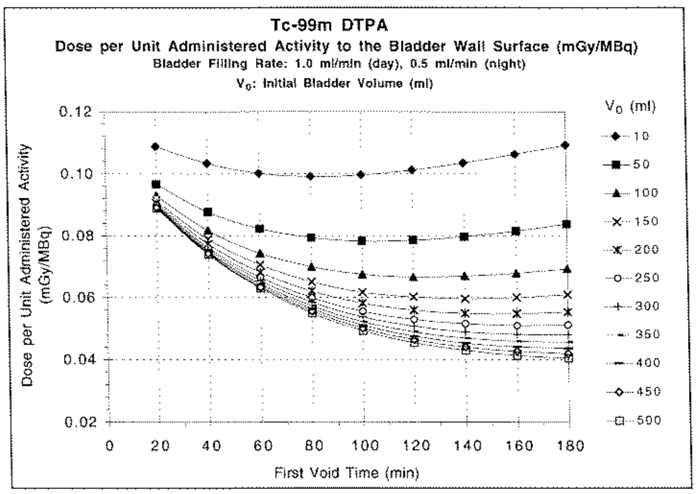

FIGURE A6. New model for ^{99m}Tc-DTPA. Dose per unit administered activity to the urinary bladder wall surface.

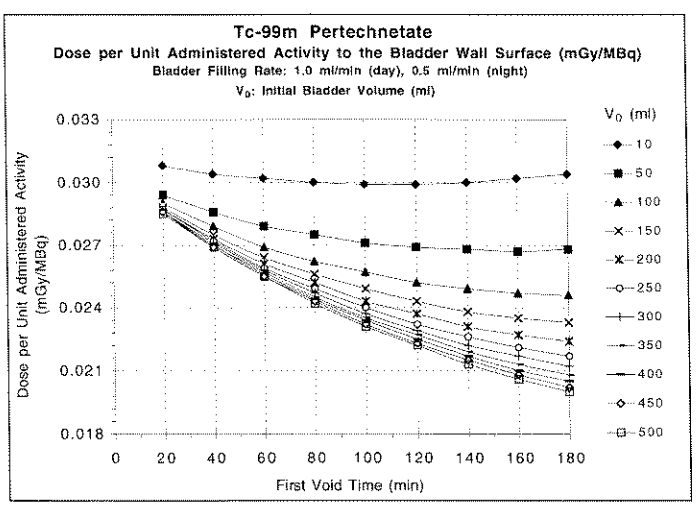

FIGURE A7. New model for ^{99m}Tc-pertechnetate. Dose per unit administered activity to the urinary bladder wall surface.

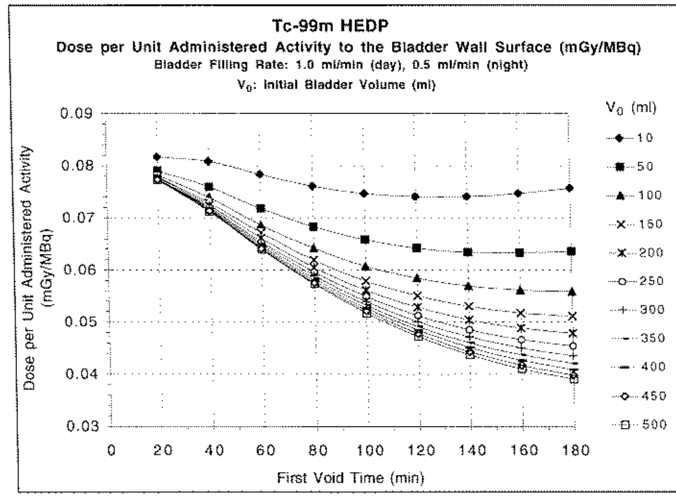

FIGURE A8. New model for ^{99m}Tc-HEDP. Dose per unit administered activity to the urinary bladder wall surface.

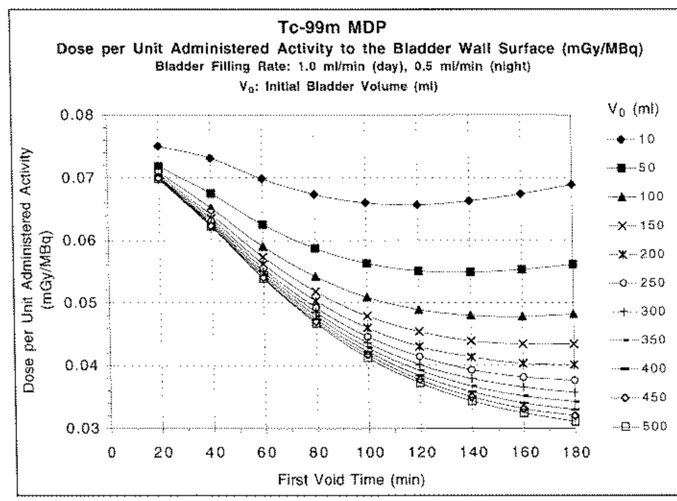

FIGURE A9. New model for ^{99m}Tc-MDP. Dose per unit administered activity to the urinary bladder wall surface.

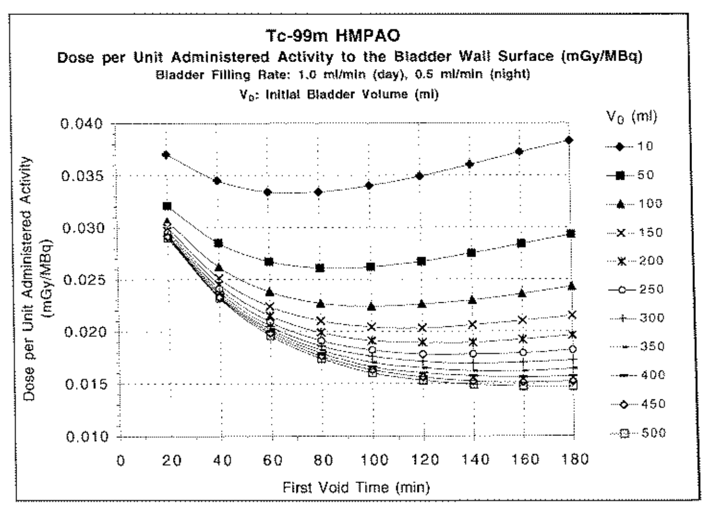

FIGURE A10. New model for ^{99m}Tc-HMPAO. Dose per unit administered activity to the urinary bladder wall surface.

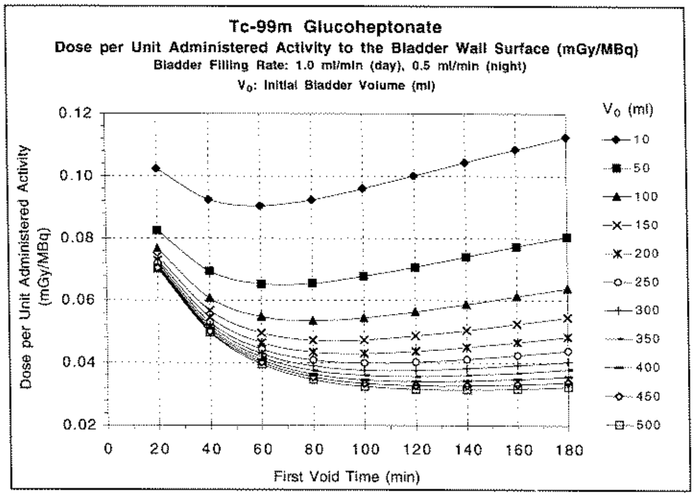

FIGURE A11. New model for ^{99m}Tc-glucoheptonate. Dose per unit administered activity to the urinary bladder wall surface.

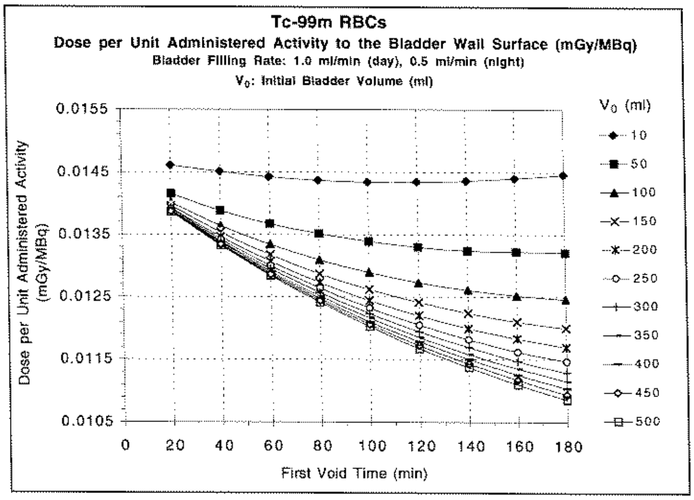

FIGURE A14. New model for ^{99m}Tc-RBCs. Dose per unit administered activity to the urinary bladder wall surface.

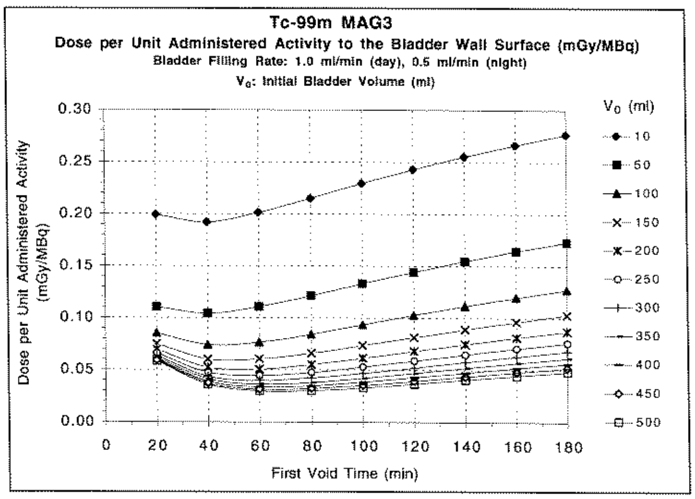

FIGURE A12. New model for ^{99m}Tc-MAG3. Dose per unit administered activity to the urinary bladder wall surface.

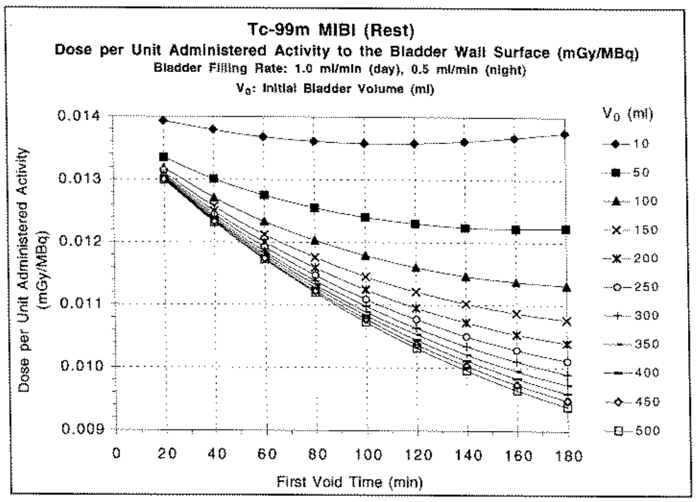

FIGURE A15. New model for ^{99m}Tc-MIBI (rest). Dose per unit administered activity to the urinary bladder wall surface.

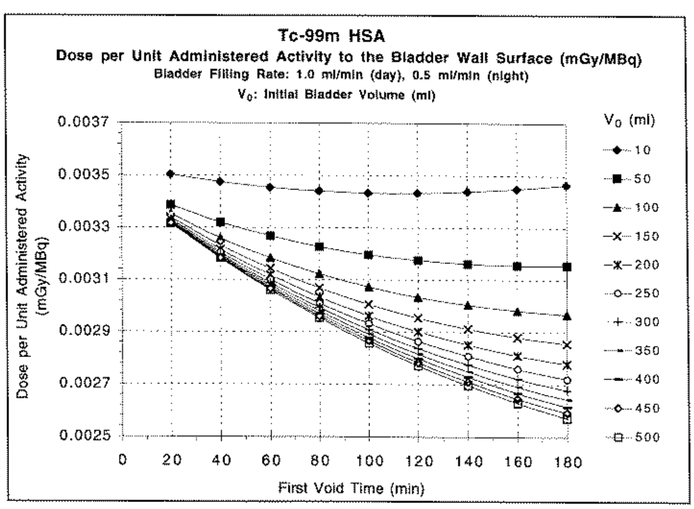

FIGURE A13. New model for ^{99m}Tc-HSA. Dose per unit administered activity to the urinary bladder wall surface.

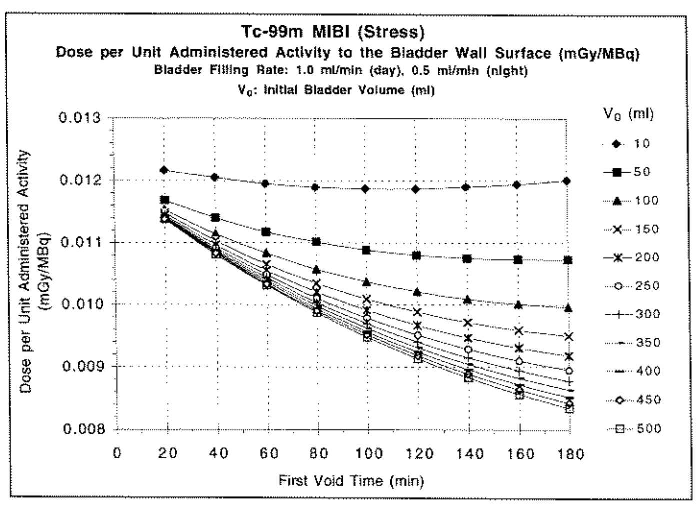

FIGURE A16. New model for ^{99m}Tc-MIBI (stress). Dose per unit administered activity to the urinary bladder wall surface.

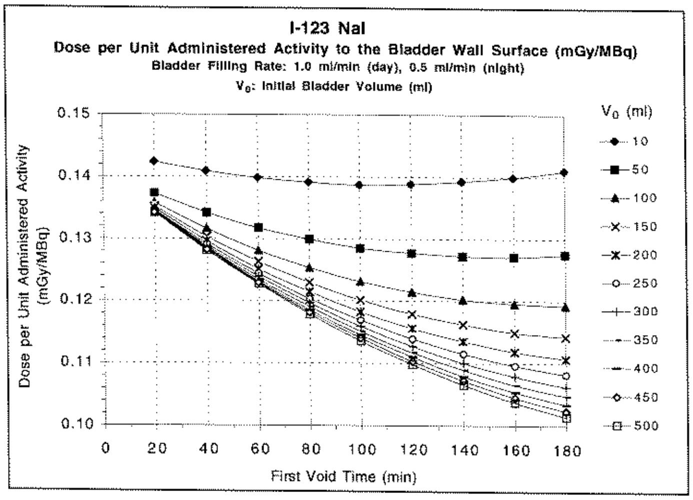

FIGURE A17. New model for ^{123}I-NaI. Dose per unit administered activity to the urinary bladder wall surface.

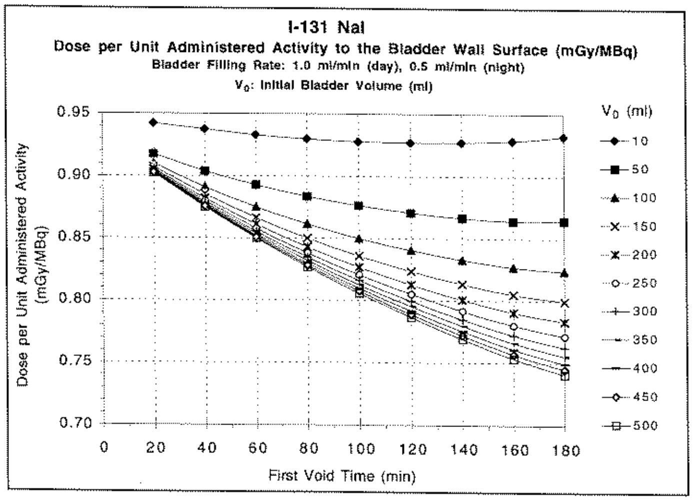

FIGURE A18. New model for ^{131}I-NaI. Dose per unit administered activity to the urinary bladder wall surface.

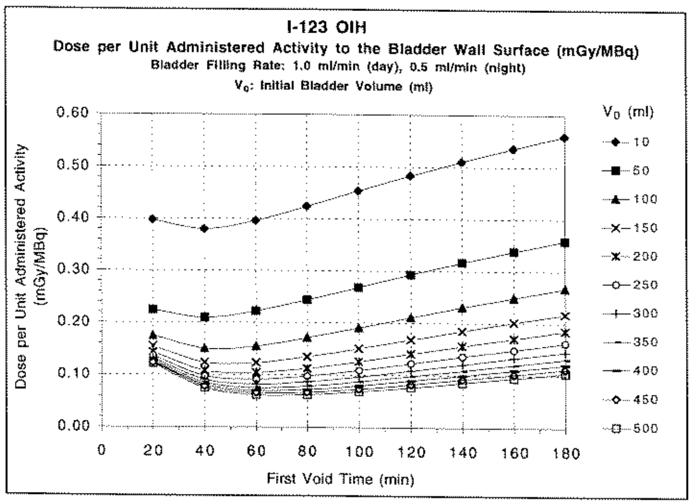

FIGURE A19. New model for ^{123}I-OIH. Dose per unit administered activity to the urinary bladder wall surface.

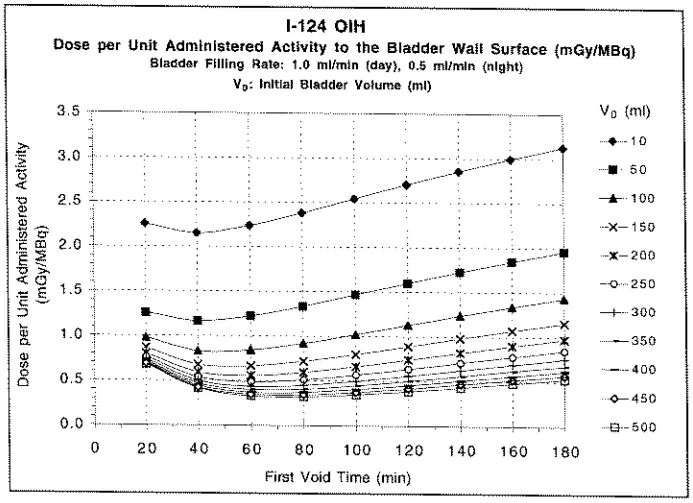

FIGURE A20. New model for ^{124}I-OIH. Dose per unit administered activity to the urinary bladder wall surface.

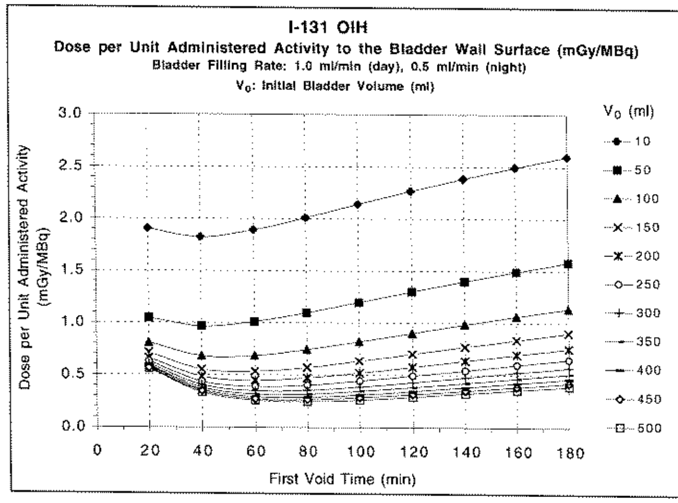

FIGURE A21. New model for ^{131}I-OIH. Dose per unit administered activity to the urinary bladder wall surface.

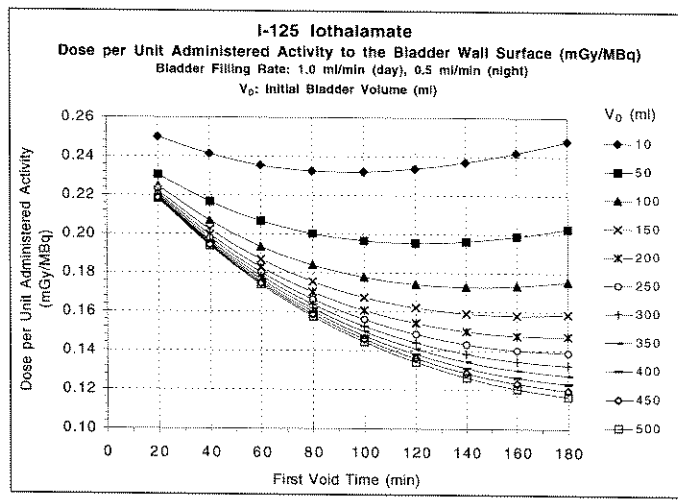

FIGURE A22. New model for ^{125}I-iothalamate. Dose per unit administered activity to the urinary bladder wall surface.

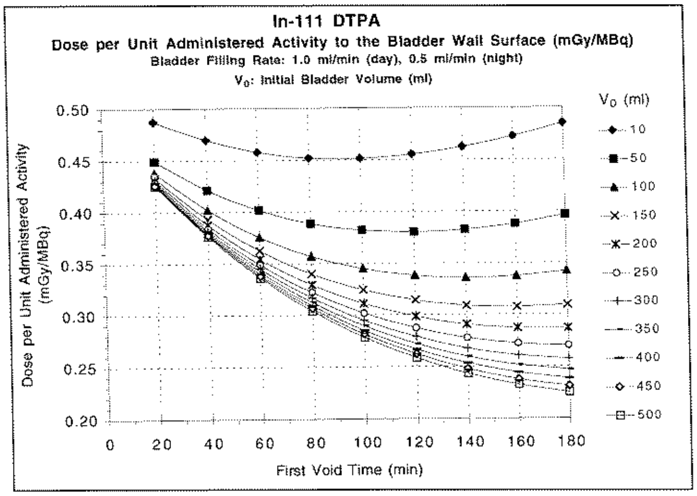

FIGURE A23. New model for ^{111}In-DTPA. Dose per unit administered activity to the urinary bladder wall surface.

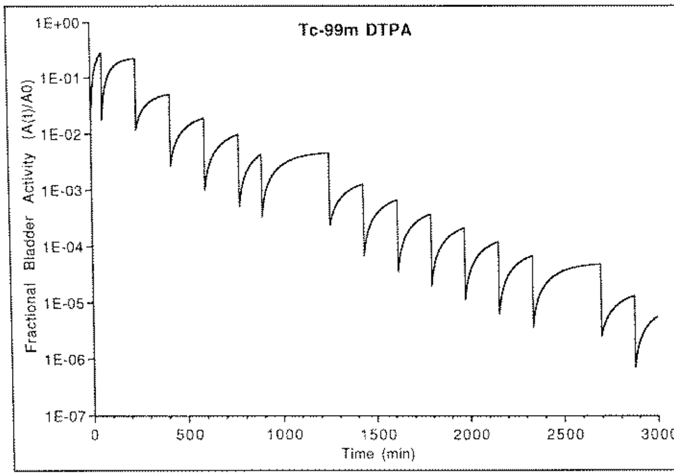

FIGURE A26. Technetium-99m-DTPA. Fractional bladder activity [A(t)/A_0 from Eq.2] as a function of time. V_0 = 100 ml, T_1 = 60 min and U(t) = 1.0/0.5 ml min^{-1} (day/night).

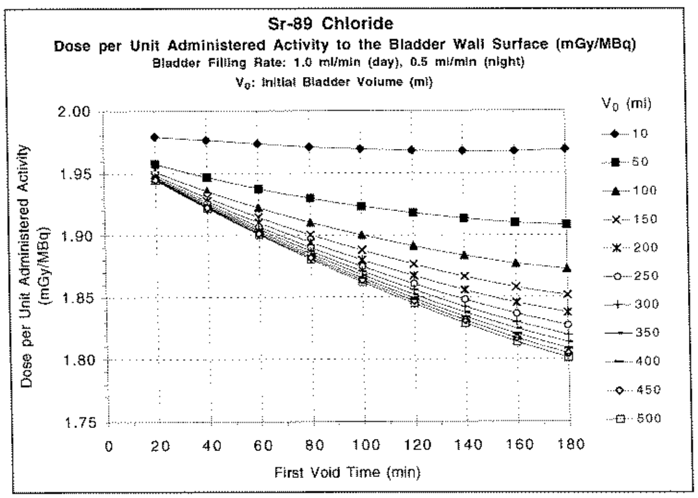

FIGURE A24. New model for ^{89}Sr-SrCl. Dose per unit administered activity to the urinary bladder wall surface.

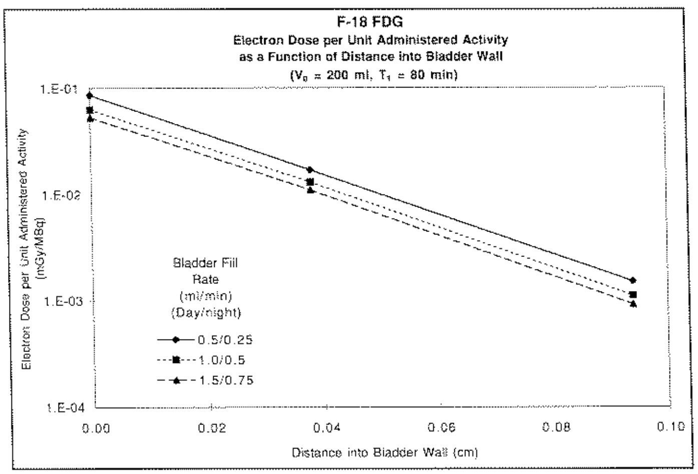

FIGURE A27. Fluorine-18-FDG. Electron dose per unit administered activity as a function of distance into the bladder wall. V_0 = 200 ml and T_1 = 60 min.

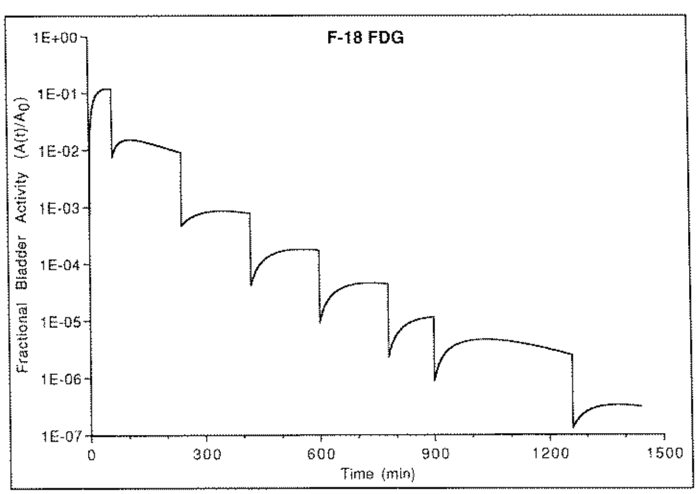

FIGURE A25. Fluorine-18-FDG. Fractional bladder activity [A(t)/A_0 from Eq. 2] as a function of time. V_0 = 100 ml, T_1 = 60 min and U(t) = 1.0/0.5 ml min^{-1} (day/night).

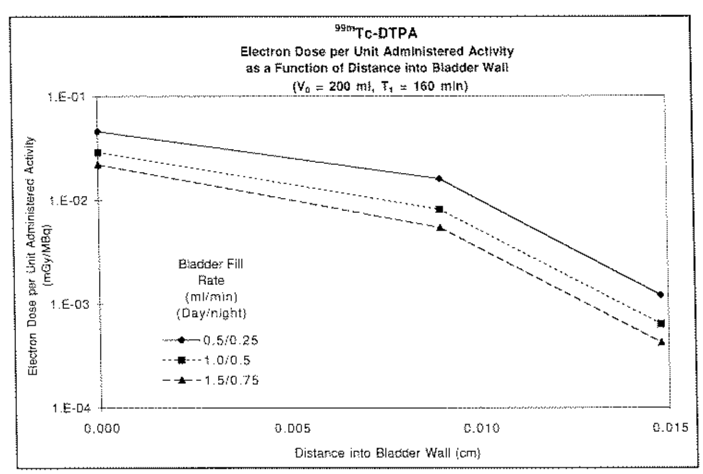

FIGURE A28. Technetium-99m-DTPA. Electron dose per unit administered activity as a function of distance into the bladder wall. V_0 = 200 ml and T_1 = 160 min.

TABLE A5
Fluorine-18-FDG
Dose per Unit Administered Activity to the Bladder Wall Surface (mGy/MBq)

	First void time (min)											
	20			60			120			180		
V_0 (ml)	(a)	(b)	(c)	(a)	(b)	(c)	(a)	(b)	(c)	(a)	(b)	(c)
10	0.61	0.35	0.24	0.54	0.31	0.23	0.60	0.36	0.26	0.65	0.40	0.29
50	0.38	0.24	0.18	0.27	0.18	0.14	0.30	0.22	0.17	0.34	0.25	0.20
100	0.33	0.21	0.16	0.19	0.13	0.11	0.20	0.15	0.13	0.23	0.18	0.15
200	0.31	0.19	0.14	0.13	0.094	0.077	0.12	0.10	0.089	0.14	0.12	0.10
500	0.29	0.18	0.13	0.091	0.063	0.051	0.066	0.055	0.050	0.073	0.064	0.059

V_0 = initial bladder volume (ml). Bladder filling rates (ml/min) were: (a) 0.5/0.25 (day/night); (b) 1.0/0.50 (day/night); and (c) 1.5/0.75 (day/night).

TABLE A6
Technetium-99m-DTPA
Dose per Unit Administered Activity to the Bladder Wall Surface (mGy/MBq)

	First void time (min)											
	20			60			120			180		
V_0 (ml)	(a)	(b)	(c)	(a)	(b)	(c)	(a)	(b)	(c)	(a)	(b)	(c)
10	0.19	0.11	0.077	0.18	0.10	0.071	0.18	0.10	0.072	0.19	0.11	0.079
50	0.17	0.097	0.070	0.14	0.082	0.060	0.13	0.079	0.059	0.13	0.084	0.064
100	0.16	0.093	0.067	0.12	0.074	0.055	0.10	0.067	0.051	0.10	0.069	0.054
200	0.16	0.091	0.066	0.11	0.068	0.050	0.087	0.056	0.043	0.080	0.055	0.045
500	0.15	0.089	0.064	0.11	0.063	0.046	0.073	0.045	0.035	0.060	0.041	0.033

V_0 = initial bladder volume (ml). Bladder filling rates (ml/min) were: (a) 0.5/0.25 (day/night); (b) 1.0/0.50 (day/night); and (c) 1.5/0.75 (day/night).

TABLE A7
Technetium-99m-Pertechnetate
Dose per Unit Administered Activity to the Bladder Wall Surface (mGy/MBq)

	First void time (min)											
	20			60			120			180		
V_0 (ml)	(a)	(b)	(c)	(a)	(b)	(c)	(a)	(b)	(c)	(a)	(b)	(c)
10	0.055	0.031	0.022	0.054	0.030	0.021	0.054	0.030	0.021	0.054	0.030	0.022
50	0.052	0.029	0.021	0.049	0.028	0.020	0.046	0.027	0.020	0.045	0.027	0.020
100	0.051	0.029	0.021	0.047	0.027	0.019	0.043	0.025	0.019	0.041	0.025	0.018
200	0.051	0.029	0.021	0.046	0.026	0.019	0.041	0.024	0.017	0.037	0.022	0.017
500	0.051	0.029	0.020	0.045	0.026	0.018	0.038	0.022	0.016	0.034	0.020	0.015

V_0 = initial bladder volume (ml). Bladder filling rates (ml/min) were: (a) 0.5/0.25 (day/night); (b) 1.0/0.50 (day/night); and (c) 1.5/0.75 (day/night).

TABLE A8
Technetium-99m-HEDP
Dose per Unit Administered Activity to the Bladder Wall Surface (mGy/MBq)

	First void time (min)											
	20			60			120			180		
V_0 (ml)	(a)	(b)	(c)	(a)	(b)	(c)	(a)	(b)	(c)	(a)	(b)	(c)
10	0.15	0.082	0.058	0.14	0.078	0.055	0.13	0.074	0.053	0.14	0.076	0.054
50	0.14	0.079	0.057	0.12	0.072	0.052	0.11	0.064	0.047	0.10	0.064	0.047
100	0.14	0.078	0.056	0.12	0.069	0.050	0.097	0.058	0.043	0.088	0.056	0.042
200	0.14	0.078	0.056	0.11	0.066	0.048	0.087	0.053	0.039	0.074	0.048	0.037
500	0.14	0.077	0.055	0.11	0.064	0.046	0.079	0.047	0.035	0.062	0.039	0.030

V_0 = initial bladder volume (ml). Bladder filling rates (ml/min) were: (a) 0.5/0.25 (day/night); (b) 1.0/0.50 (day/night); and (c) 1.5/0.75 (day/night).

TABLE A17
Iodine-123-NaI
Dose per Unit Administered Activity to the Bladder Wall Surface (mGy/MBq)

	First void time (min)											
	20			60			120			180		
V_0 (ml)	(a)	(b)	(c)	(a)	(b)	(c)	(a)	(b)	(c)	(a)	(b)	(c)
10	0.26	0.14	0.10	0.25	0.14	0.10	0.25	0.14	0.10	0.25	0.14	0.10
50	0.25	0.14	0.10	0.23	0.13	0.095	0.22	0.13	0.092	0.22	0.13	0.093
100	0.24	0.14	0.10	0.23	0.13	0.092	0.21	0.12	0.088	0.20	0.12	0.088
200	0.24	0.13	0.10	0.22	0.13	0.090	0.20	0.12	0.084	0.19	0.11	0.082
500	0.24	0.13	0.10	0.22	0.12	0.088	0.19	0.11	0.080	0.17	0.10	0.075

V_0 = initial bladder volume (ml). Bladder filling rates (ml/min) were: (a) 0.5/0.25 (day/night); (b) 1.0/0.50 (day/night); and (c) 1.5/0.75 (day/night).

TABLE A18
Iodine-131-NaI
Dose per Unit Administered Activity to the Bladder Wall Surface (mGy/MBq)

	First void time (min)											
	20			60			120			180		
V_0 (ml)	(a)	(b)	(c)	(a)	(b)	(c)	(a)	(b)	(c)	(a)	(b)	(c)
10	1.8	0.94	0.64	1.8	0.93	0.64	1.8	0.93	0.63	1.8	0.93	0.64
50	1.8	0.92	0.63	1.7	0.89	0.61	1.6	0.87	0.60	1.6	0.86	0.60
100	1.7	0.91	0.62	1.7	0.87	0.60	1.6	0.84	0.58	1.5	0.82	0.57
200	1.7	0.91	0.62	1.6	0.86	0.59	1.5	0.81	0.56	1.5	0.78	0.55
500	1.7	0.90	0.62	1.6	0.85	0.58	1.5	0.79	0.54	1.4	0.74	0.52

V_0 = initial bladder volume (ml). Bladder filling rates (ml/min) were: (a) 0.5/0.25 (day/night); (b) 1.0/0.50 (day/night); and (c) 1.5/0.75 (day/night).

TABLE A19
Iodine-123-OIH
Dose per Unit Administered Activity to the Bladder Wall Surface (mGy/MBq)

	First void time (min)											
	20			60			120			180		
V_0 (ml)	(a)	(b)	(c)	(a)	(b)	(c)	(a)	(b)	(c)	(a)	(b)	(c)
10	0.73	0.40	0.28	0.69	0.40	0.29	0.79	0.48	0.36	0.90	0.56	0.42
50	0.36	0.22	0.17	0.33	0.22	0.18	0.41	0.29	0.24	0.50	0.36	0.29
100	0.27	0.17	0.13	0.21	0.15	0.13	0.27	0.21	0.18	0.35	0.27	0.22
200	0.23	0.14	0.11	0.14	0.10	0.088	0.17	0.14	0.12	0.22	0.18	0.16
500	0.20	0.12	0.091	0.082	0.061	0.053	0.087	0.076	0.070	0.12	0.10	0.10

V_0 = initial bladder volume (ml). Bladder filling rates (ml/min) were: (a) 0.5/0.25 (day/night); (b) 1.0/0.50 (day/night); and (c) 1.5/0.75 (day/night).

TABLE A20
Iodine-124-OIH
Dose per Unit Administered Activity to the Bladder Wall Surface (mGy/MBq)

	First void time (min)											
	20			60			120			180		
V_0 (ml)	(a)	(b)	(c)	(a)	(b)	(c)	(a)	(b)	(c)	(a)	(b)	(c)
10	4.3	2.3	1.5	4.0	2.2	1.6	4.6	2.7	2.0	5.2	3.1	2.3
50	2.1	1.3	0.93	1.9	1.2	1.0	2.3	1.6	1.3	2.8	2.0	1.5
100	1.6	1.0	0.73	1.2	0.84	0.68	1.5	1.1	0.93	1.9	1.4	1.2
200	1.3	0.80	0.60	0.77	0.56	0.46	0.93	0.74	0.64	1.2	1.0	0.84
500	1.1	0.68	0.50	0.46	0.33	0.27	0.45	0.39	0.35	0.61	0.53	0.48

V_0 = initial bladder volume (ml). Bladder filling rates (ml/min) were: (a) 0.5/0.25 (day/night); (b) 1.0/0.50 (day/night); and (c) 1.5/0.75 (day/night).

TABLE A21
Iodine-131-OIH
Dose per Unit Administered Activity to the Bladder Wall Surface (mGy/MBq)

	First void time (min)											
	20			60			120			180		
V_0 (ml)	(a)	(b)	(c)	(a)	(b)	(c)	(a)	(b)	(c)	(a)	(b)	(c)
10	3.7	1.9	1.3	3.4	1.9	1.3	3.9	2.3	1.6	4.4	2.6	1.9
50	1.8	1.0	0.76	1.6	1.0	0.78	1.9	1.3	1.0	2.3	1.6	1.2
100	1.3	0.81	0.60	1.0	0.68	0.55	1.2	0.90	0.74	1.6	1.1	0.93
200	1.1	0.66	0.49	0.63	0.45	0.37	0.74	0.58	0.49	1.0	0.75	0.64
500	1.0	0.56	0.41	0.37	0.26	0.21	0.35	0.29	0.26	0.46	0.39	0.35

V_0 = initial bladder volume (ml). Bladder filling rates (ml/min) were: (a) 0.5/0.25 (day/night); (b) 1.0/0.50 (day/night); and (c) 1.5/0.75 (day/night).

TABLE A22
Iodine-125-Iothalamate
Dose per Unit Administered Activity to the Bladder Wall Surface (mGy/MBq)

	First void time (min)											
	20			60			120			180		
V_0 (ml)	(a)	(b)	(c)	(a)	(b)	(c)	(a)	(b)	(c)	(a)	(b)	(c)
10	0.45	0.25	0.18	0.43	0.24	0.17	0.42	0.23	0.17	0.44	0.25	0.18
50	0.41	0.23	0.17	0.36	0.21	0.15	0.33	0.20	0.14	0.33	0.20	0.15
100	0.40	0.22	0.16	0.33	0.19	0.14	0.28	0.17	0.13	0.27	0.18	0.14
200	0.39	0.22	0.16	0.32	0.18	0.13	0.25	0.15	0.12	0.22	0.15	0.12
500	0.39	0.22	0.16	0.30	0.17	0.13	0.22	0.13	0.10	0.18	0.12	0.092

V_0 = initial bladder volume (ml). Bladder filling rates (ml/min) were: (a) 0.5/0.25 (day/night); (b) 1.0/0.50 (day/night); and (c) 1.5/0.75 (day/night).

TABLE A23
Indium-111-DTPA
Dose per Unit Administered Activity to the Bladder Wall Surface (mGy/MBq)

	First void time (min)											
	20			60			120			180		
V_0 (ml)	(a)	(b)	(c)	(a)	(b)	(c)	(a)	(b)	(c)	(a)	(b)	(c)
10	0.87	0.49	0.35	0.83	0.46	0.33	0.81	0.46	0.33	0.85	0.48	0.35
50	0.78	0.45	0.33	0.69	0.40	0.29	0.63	0.38	0.28	0.63	0.40	0.30
100	0.76	0.44	0.32	0.64	0.38	0.28	0.54	0.34	0.26	0.52	0.34	0.27
200	0.75	0.43	0.31	0.60	0.35	0.26	0.48	0.30	0.23	0.43	0.29	0.23
500	0.74	0.43	0.31	0.58	0.34	0.25	0.42	0.26	0.20	0.34	0.23	0.18

V_0 = initial bladder volume (ml). Bladder filling rates (ml/min) were: (a) 0.5/0.25 (day/night); (b) 1.0/0.50 (day/night); and (c) 1.5/0.75 (day/night).

TABLE A24
Strontium-89-Chloride
Dose per Unit Administered Activity to the Bladder Wall Surface (mGy/MBq)

	First void time (min)											
	20			60			120			180		
V_0 (ml)	(a)	(b)	(c)	(a)	(b)	(c)	(a)	(b)	(c)	(a)	(b)	(c)
10	3.9	2.0	1.3	3.9	2.0	1.3	3.9	2.0	1.3	3.9	2.0	1.3
50	3.9	2.0	1.3	3.8	1.9	1.3	3.8	1.9	1.3	3.7	1.9	1.3
100	3.9	2.0	1.3	3.8	1.9	1.3	3.7	1.9	1.3	3.7	1.9	1.3
200	3.9	1.9	1.3	3.8	1.9	1.3	3.7	1.9	1.3	3.6	1.8	1.2
500	3.8	1.9	1.3	3.8	1.9	1.3	3.6	1.8	1.2	3.5	1.8	1.2

V_0 = initial bladder volume (ml). Bladder filling rates (ml/min) were: (a) 0.5/0.25 (day/night); (b) 1.0/0.50 (day/night); and (c) 1.5/0.75 (day/night).

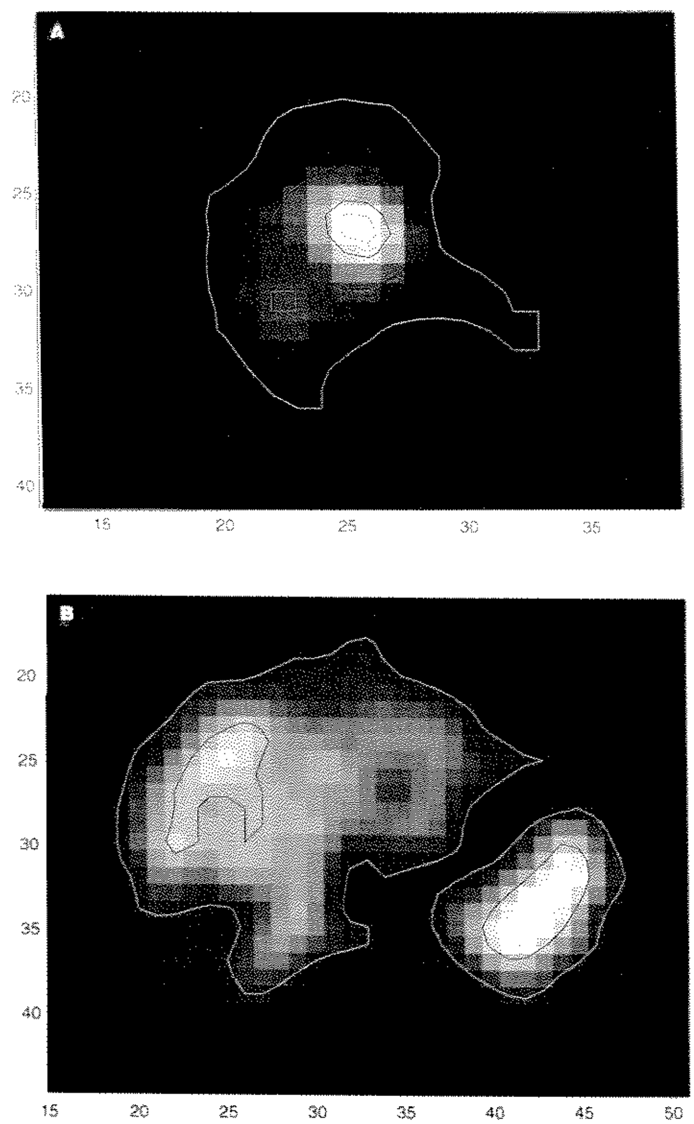

FIGURE 8. Bremsstrahlung SPECT images from a 629 MBq injection of colloidal ^{32}P chromic phosphate in the liver of patient with nonresectable liver metastates. (a) SPECT Slice 3, showing maximal localization of activity. (b) SPECT Slice 10, showing unintended transfer of activity to the spleen. Relative isodose curves are shown for 10% (yellow), 30% (magenta), 50% (blue), 70% (red) and 90% (green) of the maximum voxel dose estimated to be 415 Gy. Pixel locations are indicated for both abscissa and ordinate.

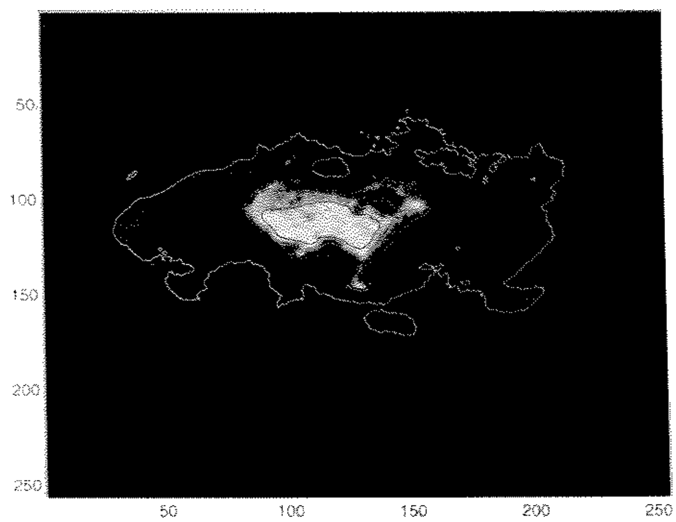

FIGURE 11. Distribution of ^{131}I monoclonal antibody within an A6H tumor xenograft (mouse renal cell carcinoma) as determined by implanted micro-TLDs. Relative isodose contours within the tumor are shown as determined by the MIRD schema using ^{131}I voxel S values for voxels 50 μm × 50 μm × 1 mm in dimension. Curves are shown for 10% (yellow), 30% (magenta), 50% (blue), 70% (red) and 90% (green) of the maximum voxel dose estimated to be 14.4 Gy. Pixel locations are indicated for both abscissa and ordinate.

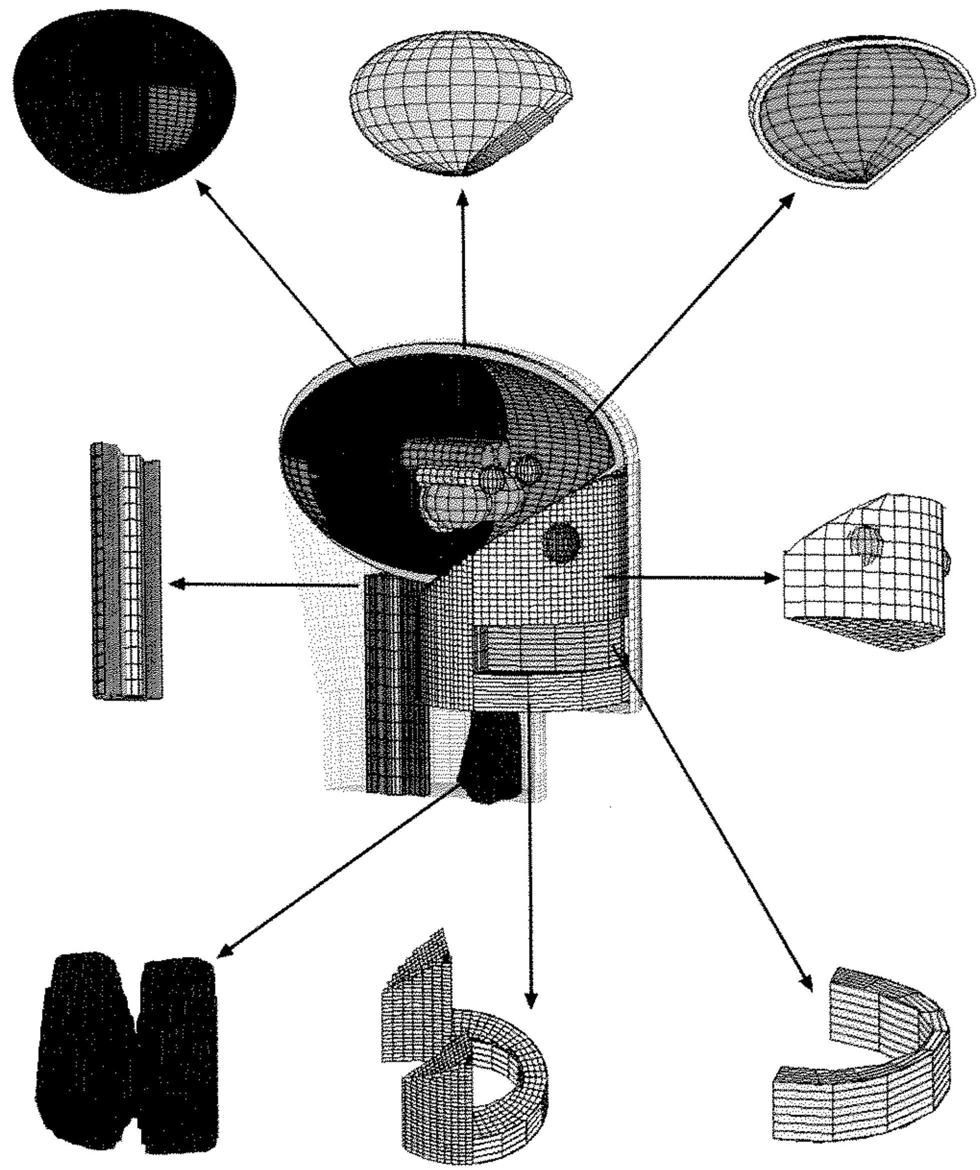

FIGURE 3. Interior features of the new MIRD head and brain model of the adult. Eight components of the model are also shown, which include (Upper Middle) an exterior view of the cranium; (Upper Left) an interior view of the cranium (brain excluded); (Center Left) the upper facial region and eyes; (Lower Left) the teeth; (Lower Middle) the mandible; (Lower Right) the thyroid; (Center Right) the three-region spine; and (Upper Right) the cerebral cortex (red) and cerebellum (blue).

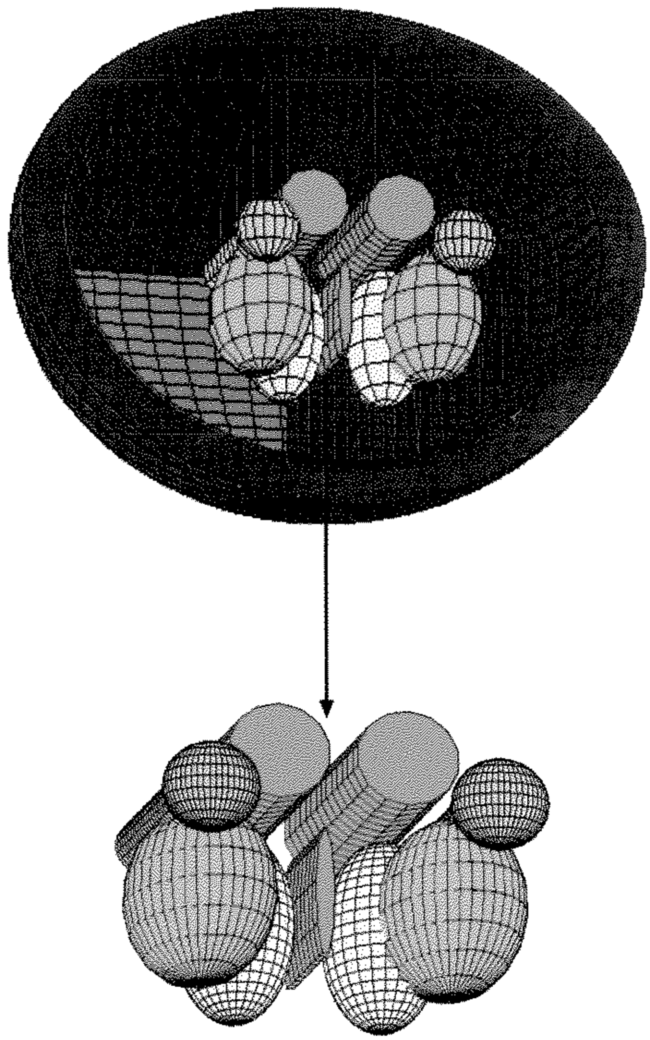

FIGURE 4. Interior features of the new MIRD brain model (coronal section viewing the posterior region of the brain). The subregions modeled include the cerebral cortex (red), the cerebellum (dark blue), the thalami (light blue), the ventricles (green), caudate nuclei (pink) and the lentiform nuclei (yellow). To view the cerebellum, a coronal slice through the cerebral cortex was made, and the layer of cerebral cortex covering the cerebellum has been removed.